

Pinching Sudakov

A.V. Belitsky,^a L.V. Bork,^b V.A. Smirnov^c

^a*Department of Physics, Arizona State University, Tempe, AZ 85287-1504, USA*

^b*Institute for Theoretical and Experimental Physics, 117218 Moscow, Russia*

The Center for Fundamental and Applied Research, 127030 Moscow, Russia

^c*Skobeltsyn Institute of Nuclear Physics, Moscow State University 119992 Moscow, Russia*

ABSTRACT: In this paper, we discuss the factorization of the Sudakov form factor on the Coulomb branch of maximally supersymmetric Yang-Mills theory in the near mass-shell limit. We unravel all pinch singularities of this observable making use of the Method of Regions. We find their operator content in terms of matrix elements of Wilson lines on semi-infinite and finite intervals for the jet and ultrasoft functions, respectively. However, naive factorization into these incoherent momentum components is broken at two-loop order by effects subleading in the parameter of dimensional regularization. To save the day, we perform an appropriate twisting of the functions involved as well as simultaneous finite scheme transformation of the 't Hooft coupling. Infrared physics of twisted jet and ultrasoft functions is governed by the octagon anomalous dimension, while the untwisted ultrasoft function possesses infrared evolution driven by an anomalous dimension different from the ubiquitous cusp.

Contents

1	Introduction	2
2	Off-shell Sudakov form factor	4
3	MofR assisted factorization	7
3.1	Geometric approach to MofR	8
3.2	One-loop: MofR and pinching	10
4	Jet function: definition and one-loop result	12
5	Ultrasoft function	14
5.1	Definition	14
5.2	Perturbative expansion: One loop	16
5.3	Two loops	17
5.3.1	Ladder graphs	17
5.3.2	Non-Abelian graphs	18
5.3.3	Self-energy graphs	19
5.3.4	The sum	20
6	All-order factorization: a proposal	20
7	Two-loop test	21
7.1	MofR vs. naive factorization	21
7.2	Twisted functions and finite renormalization	24
8	Evolution equations	25
8.1	Renormalization group	25
8.2	Infrared evolution	26
8.3	Untwisted vs. twisted	27
9	Conclusions	27
A	Light-cone singularity of scalar propagator	28
B	Region integrals at two loops	29

1 Introduction

Quantum-mechanical independence of physics happening at different space-time or momentum scales is at the heart of factorization theorems which form, in turn, the foundation for quantitative applications of QCD to particle phenomenology. Factorization of a full amplitude into its incoherence components intrinsically introduces an arbitrary scale into the problem. Then the statement of independence of the former on the latter translates into the renormalization group equations. These equations allow one to perform an effective resummation of large corrections to all orders of perturbation theory. They stem from logarithms of ratios of the aforementioned different distance scales. The only first-principle ingredients required to accomplish this goal are the anomalous dimensions.

Some time ago [1], we proposed an exact formula for the near mass-shell Sudakov form factor in the maximally supersymmetric Yang-Mills there, aka $\mathcal{N} = 4$ sYM, based on a direct three-loop calculation [2] as well as complimentary information from four-point correlation functions of infinitely heavy BPS operators [3]. The formula admits a stunningly simple form both in the 't Hooft coupling and in the kinematical $m^2 \equiv P^2/q^2$ invariant involved as $m \rightarrow 0$,

$$\log \mathcal{F}_2 = -\frac{1}{2}\Gamma_{\text{oct}}(g) \log^2 m^2 - D(g), \quad (1.1)$$

with

$$\Gamma_{\text{oct}}(g) = \frac{2}{\pi^2} \log \cosh(2\pi g), \quad D(g) = \frac{1}{4} \log \frac{\sinh(4\pi g)}{4\pi g}, \quad (1.2)$$

where the coefficient accompanying the double logarithm is known as the octagon anomalous dimension. This result appears to clash with folklore wisdom that all infrared-sensitive physics in gauge theories is driven by the so-called cusp anomalous dimension. The one-loop result displays a well-known factor-of-two difference between the on- and off-shell kinematics [4, 5], see also [6] for a nice historical exposition¹. A factorization formula for this observable within QCD was suggested almost four decades ago [5]. However, it refers only to the cusp and no trace of the octagon anomalous dimension can be found there. So how do we reconcile these? With the unfactorized form factor displaying such a simple form, does its separation into soft and collinear degrees of freedom obscure its simplicity such that it is gone at the end? Does this suggest that factorization is violated?

Most of the time, factorization is discussed in generic terms based on Landau equations [7] via Coleman-Norton adaptation [8] and deducing corresponding pinch surfaces where singularities of various momentum modes reside. However, this is rarely done with support from explicit (multi) loop calculations. Here we go in the opposite direction. We have an exact answer for the form factor and diagrammatic representation for the lowest few orders of perturbation theory. The latter is encoded in a small set of scalar integrals corresponding to sums of the original Feynman graphs making use of Passarino-Veltman reductions. In

¹We would like to thank Lorenzo Magnea for drawing our attention to this paper.

fact, in the case at hand, these expressions were fast-tracked to their concise form making use of unitarity-based techniques. So our starting point will not be a diagram-by-diagram basis but rather a small set of scalar integrals.

Our consideration in this paper will be based on the Method of Regions (MofR) [9], see Ref. [10] for a concise review. This formalism, though carries on a label of experimental mathematics, had proven itself in the past to provide correct results for asymptotic expansions of various observables, cross sections, and scattering amplitudes alike. MofR will provide us with a bare, i.e., before renormalization, form of the factorization formula we are looking for. The formalism provides an exact mapping of regions to pinch surfaces encoded in Landau equations. Our attachment to the method will immediately imply however that our factorization formula will be oblivious to certain incoherent components of the factorized result. Namely, since dimensional regularization/reduction is indispensable for a robust and proper treatment of different regions of the phase space, zero-bin effects [11, 12] will be invisible to us. This is a mere consequence of the fact that scaleless integrals identically vanish within it. However, the upside is that MofR gives a precise definition to contributing Feynman integrals in various momentum regions inherit the intrinsic property of the method: all loop-momentum integrals are unrestricted and cover the entire Minkowski space rather than a subspace with proper momentum scalings as practiced in certain approaches to factorization. This feature will offer us a way to uncover their operator definitions in terms of local fields and extended objects like Wilson lines. These can then be computed from the conventional Feynman diagram technique and compared with results from MofR.

Let us point out an advantage of applying MofR to the off-shell Sudakov form factors, compared to its on-shell counterpart. Factorization theorem for the latter was repeatedly discussed in the literature over the past forty years, see [13] for a thorough recent review, and are summarized in the following formula [12]

$$\mathcal{F}_2^{\text{on-shell}} = H(J_1/J_1^{\text{eik}})(J_2/J_2^{\text{eik}})S, \quad (1.3)$$

where J_i and J_i^{eik} are the jet functions [14] and their eikonal versions [12], respectively, S is the soft function determined by the vacuum expectation value of semi-infinite Wilson lines meeting at a cusp [15], and, last but not least, H is the hard matching coefficient. With the use of conventional dimensional regularization to tame both ultraviolet and infrared divergences, all quantum corrections to on-shell case matrix elements of operators built solely from Wilson lines vanish identically since they are given in terms of scaleless momentum integrals. On the one hand, it manifests the equivalence of infrared and ultraviolet effects in these functions, which was one of the reasons for using the renormalization group of Wilson lines for studies of the infrared physics of amplitudes [15]. However, it then requires a clean separation between the two, and therefore, there is a necessity to rely on a regularization for infrared physics that is different from dimensional. In this manner, the eikonal functions become given by counterterms [16]. On the other hand, if one entirely relies on dimensional regularization, which does the job perfectly, then the soft function and the eikonal jets are simply one. With this perfectly valid point of view, the soft effects migrate elsewhere in the

above factorization formula, as was done multiple times in the past [17, 18]. However, in this manner MofR “throws the baby out with the tubwater” as one of the important ingredients of infrared physics becomes a collateral of the formalism. None of these is the case for the off-shell Sudakov since the external virtuality introduces an intrinsic scale in majority of matrix elements involving Wilson lines and so we can clearly identify all momentum components in the factorization formula analogous to (1.3) for \mathcal{F}_2 except for the eikonal jets (zero-bin subtractions). However, This will suffice for the goals we set up in this work.

Our subsequent presentation is organized as follows. In the next section, we recall the definition of the Sudakov form factor and the basis scalar integrals defining its two-loop form. Next, in Sect. 3, we review the geometric approach to MofR and apply it to the one-loop Sudakov form factor in the near mass-shell limit. We use these one-loop results to propose an operator definition for the jet and ultrasoft functions which define leading pinched regions as $m \rightarrow 0$. In Sect. 4, we evaluate the jet function to one loop order using its definition as an amputated off-shell Green function of a semi-infinite Wilson line on the light cone. In Sect. 5.1, we define the ultrasoft function and, then, calculate it in Sect. 5.2 and 5.3 to one- and two-loop order, respectively. In Sect. 6, we conjecture a factorized form of the near mass-shell Sudakov form factor akin to Eq. (1.3) in the on-shell case. Then, we turn to its verification at two-loop order making use of MofR in Sect. 7. We verify there the equivalence of the ultrasoft region stemming from MofR to the one from the operator definition of the function in question. However, we encounter difficulties with the suggested naive factorization formula. Namely, while the effects of $O(\varepsilon)$ are irrelevant for the complete off-shell factor: the form factor is finite for $P_i^2 \neq 0$ and ε can be set to zero in the sum, its individual factorized components are highly sensitive to these effects in order to enforce an agreement with the full expression. As we will demonstrate in Sect. 7.2, a slight mismatch between the product of the one-loop collinear and soft contributions and their two-loop counterpart forces us to ‘twist’ the definitions of individual momentum components and also to perform a finite scheme transformation of the ’t Hooft coupling. These steps change the form of the infrared evolution equations for the ultrasoft-collinear functions involved. Finally, we conclude. Two appendices contain supplementary material needed for a better understanding of the main body of the paper.

2 Off-shell Sudakov form factor

The main object of our current analysis is the off-shell Sudakov form factor² in the $\mathcal{N} = 4$ sYM

$$\frac{1}{2N_c} \int d^4x e^{-iq \cdot x} \langle P_1, P_2 | \text{tr}_{\text{adj}} \phi_{12}^2(x) | 0 \rangle_{\text{amp}} = (2\pi)^4 \delta^{(4)}(q - P_1 - P_2) \mathcal{F}_2, \quad (2.1)$$

where $\phi = \phi_{12}$ of the sextet ϕ_{AB} of scalars of the $\mathcal{N} = 4$ sYM and, unless stated otherwise, all fields are adjoint matrices $\phi = \phi_a T^a$ with the generators defined by the $\text{SU}(N_c)$ structure

²Notice with our definition of amputated states, the form factor \mathcal{F}_2 is dimensionless.

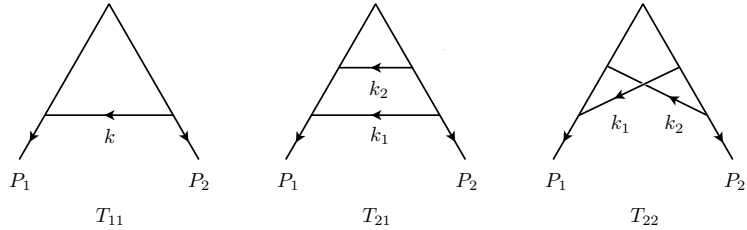


Figure 1. Scalar integrals defining the two-loop form factor.

constants $(T^a)^{bc} = -if^{abc}$. The composite operator ϕ_{12}^2 defining it is BPS and thus the matrix element on its left-hand side is ultraviolet finite. For finite virtualities $P_i^2 \neq 0$, it is infrared finite as well. It was claimed in the literature [19] that these virtualities can be generated in a gauge invariant manner by considering maximally supersymmetric theory in higher dimensions while restricting loop integrals to four dimensions only. Higher dimensional components of external momenta will play the role of virtualities for momenta P_i [19]. This approach is equivalent to consideration of the $\mathcal{N} = 4$ sYM on the Coulomb branch [19, 20]. Integrands of the Sudakov form factor are expected to be universal in all dimensions [21], so to obtain the form factor \mathcal{F}_2 on the Coulomb branch, i.e., the off-shell form factor we can use the naive off-shell continuation of on-shell result in $\mathcal{N} = 4$ sYM from the work of van Neerven from almost four decades ago [22] (see also more recent [21, 23]). According to this analysis, up to two-loop order, the perturbative expansion of \mathcal{F}_2 can be expressed in terms of just one and two scalar integrals at corresponding loop orders after Passarino-Veltman tensor reduction

$$\mathcal{F}_2 = 1 + g^2[-2T_{11}] + g^4[4T_{21} + T_{22}] + O(g^6). \quad (2.2)$$

They are the (iterated) ladders T_{11} , T_{21} and the cross ladder T_{22} , as shown in Fig. 1,

$$T_{11} = q^2 \int_k D(k)D(k - P_1)D(k + P_2), \quad (2.3)$$

$$T_{21} = q^4 \int_{k_1, k_2} D(k_1)D(k_2)D(k_1 - P_1)D(k_1 + k_2 - P_1)D(k_1 + P_2)D(k_1 + k_2 + P_2), \quad (2.4)$$

$$T_{22} = q^4 \int_{k_1, k_2} D(k_1)D(k_2)D(k_1 - P_1)D(k_1 + k_2 - P_1)D(k_2 + P_2)D(k_1 + k_2 + P_2), \quad (2.5)$$

built from the products of the scalar propagators $D(k) = [k^2 + i0]^{-1}$. The original analysis in Ref. [22] was performed for massless on-shell legs $P_i^2 = 0$ [24] as distinguished it from its off-shell counterpart in the original Sudakov's treatment [25], one needs to tame infrared divergences. A version of dimensional regularization known as the supersymmetry-preserving dimensional reduction [26] was employed there [22]. So the above perturbative series is cast in terms of the D -dimensional 't Hooft coupling (with g_{YM} being the dimensionless bare

Yang-Mills coupling constant)

$$g^2 \equiv e^{-\varepsilon\gamma_E} \frac{g_{\text{YM}}^2 N_c}{(4\pi)^{D/2}}, \quad (2.6)$$

and the D -dimensional loop-momentum integrations are performed with the $\overline{\text{MS}}$ -measure

$$\int_k \equiv e^{\varepsilon\gamma_E} \mu^{2\varepsilon} \int \frac{d^D k}{i\pi^{D/2}}, \quad (2.7)$$

where $D \equiv 4 - 2\varepsilon$. In spite of the fact that in our analysis the external lines are taken off the mass shell and thus the infrared singularities are regularized by $P_i^2 \neq 0$, we will adopt the same D -dimensional notations as given above since factorization of these finite integrals in terms of individual momentum regions inevitably and unavoidably induces divergences that need proper regularization. These will be of different nature depending on the assumed sign of the ε parameter, either ultraviolet or infrared as we will see below. But all of them will be unequivocally regularized by going to $D \neq 4$ dimensions.

In our earlier studies [1, 2], we calculated the off-shell Sudakov form factor up to three-loop order, i.e., an order of perturbation theory higher than displayed in Eq. (2.2). We found that, for Euclidean external kinematics³, in the near mass-shell limit

$$q^2 = -Q^2 < 0, \quad P_i^2 = -m^2 < 0, \quad m^2/Q^2 \ll 1, \quad (2.8)$$

it exponentiates as shown in Eq. (1.1) including finite terms. Here, we expanded the exact results to $O(g^6)$,

$$\Gamma_{\text{oct}}(g) = 4g^2 - 16\zeta_2 g^4 + \dots, \quad D(g) = 4\zeta_2 g^2 - 32\zeta_4 g^4 + \dots \quad (2.9)$$

In the present study, we will dissect this result and stitch its various momentum components back together à la factorization theorem.

Our considerations in Refs. [1, 2] were based on two independent formalisms. One was grounded in a rigorous technique of deriving a Fuchsian system of linear differential equations [27] for a set of the so-called Master Integrals (MIs) and solving the former interactively order by order in ε . The scalar integrals T_{ij} defining the form factor were then reduced to these MIs by employing integration-by-parts identities. The asymptotic limit of the near on-shell limit was taken only at the very end of the calculation. Another technique that we employed was far less robust. It carries on the status of experimental mathematics. It is known under the name of the Method of Regions (MofR) [9]. It consists of determining all non-overlapping regions of loop-momentum integrations scaling appropriately with external kinematical limits imposed on observables in question, Taylor expanding integrands

³By extracting the overall mass dimension of the form factor in terms of Q^2 , \mathcal{F}_2 becomes a function of the ratio m^2/Q^2 only. So without loss of generality, we will set $Q^2 = 1$ from now on. This implies that all scalar integrals T_{ij} are functions of the small variable m only, $T_{ij} = T_{ij}(m)$ (and, away from $D = 4$, of μ measured in units of Q).

of Feynman integrals according to these and finally integrating every one of them over the *entire* momentum space, dropping scaleless integrals along the way. Using this technique we recovered the result of the differential equations, thus, putting MofR on a firmer foundation for the problem at hand. It was shown that overlap contributions usually yield scaleless integrals which can be set to zero if they are regulated appropriately [28].

In the present study, the MofR takes center stage!

3 MofR assisted factorization

Traditionally factorization of multiscale Green's functions/matrix elements in terms of incoherent components responsible for physics at different momentum scales is accomplished by means of perturbative analysis of Feynman graphs' integrands making use of Landau equations [7, 29, 30]. The latter are most straightforwardly formulated by employing Feynman parametrization of momentum integrals. Since this will be our main technical tool, it only makes more sense to introduce it early.

Namely, for the L_{ij} -loop integrals in Eqs. (2.3)-(2.5), we define

$$T_{ij}(m) = \int_0^\infty d^{N_{ij}} \mathbf{x} \mathcal{J}_{N_{ij}, L_{ij}}(\mathbf{x}; m), \quad (3.1)$$

with the integration measure and the integrand given by

$$d^N \mathbf{x} = \prod_{i=1}^N dx_i \delta\left(\sum_{i=1}^N x_i - 1\right), \quad \mathcal{J}_{N,L}(\mathbf{x}; m) = \int_{k_1, \dots, k_L} \frac{\Gamma(N)}{\left[-\sum_{i=1}^N x_i D_i^{-1}\right]^N}, \quad (3.2)$$

respectively. A parameter x_i is associated with each (inverse) Feynman propagator D^{-1} so that N_{ij} is their total number in a given graph.

Making use of these definitions, infrared singularities of Feynman integrals are determined by the Landau equations

$$x_i D_i^{-1} = 0, \quad \partial_{k_\ell} \sum_{i=1}^N x_i D_i^{-1} = 0. \quad (3.3)$$

The first of them states that infrared singularities of Feynman integrals stem either when each propagator in a graph goes on-shell or when the corresponding line is eliminated from it. The second condition implies that the integration contours cannot be deformed away from these singularities and thus they get *pinched* by them. Every set of solutions to the Landau equations provides a *pinched surface* where singularities reside and thus endow every Feynman graph with its reduced counterpart. However, our pinching will be a little bit more specific than traditional analyses [29] in that every component of the reduced graph will have a precise operator definition involving *unrestricted* integration over the entire momentum space. In this sense, our treatment is akin to the one performed with the framework of effective field theories [31, 32] or more recent approaches to on-shell physics [12, 13]. However, the use of different regularization procedures will trickle down to differences in the form of factorized components involved.

3.1 Geometric approach to MofR

MofR formulated in the momentum space, as described at the end of Sect. 2, can be quite tedious when applied to multiloop integrals [33] due to the necessity to cover the entire range of loop momenta with non-overlapping regions even though sometimes these generate scaleless integrals that vanish within dimensional regularization [28]. Here is where the Feynman parametrization comes to the rescue again, as was demonstrated in Ref. [34]. It was shown there that all non-vanishing regions can be formulated in a covariant fashion independent of such nuisances as a choice of reference frame or loop-momentum routing within a graph. In addition, the Feynman integral representation (up to a stipulation to be pointed below) allows one for an entirely geometric way to unravel contributing regions [35].

It proceeds as follows [35], see also recent Refs. [36, 37], for more comprehensive, reader-friendly treatments. Integrating out the loop momenta in the Feynman integrand (3.2), it is cast in terms of two Symanzik polynomials U and F ,

$$\mathcal{J}_{N,L}(\mathbf{x}; m) = e^{\varepsilon\gamma_E L} \mu^{2\varepsilon L} \Gamma\left(N - \frac{1}{2}LD\right) [U(\mathbf{x})]^{N - \frac{1}{2}(L+1)D} [F(\mathbf{x}; m)]^{-N + \frac{1}{2}LD}, \quad (3.4)$$

with U/F being independent of/dependent on the kinematical invariant m and determined by the spanning trees (T^1)/two-trees (T^2),

$$U(\mathbf{x}) = \sum_{T^1} \prod_{i \notin T^1} x_i, \quad F(\mathbf{x}; m) = - \sum_{T^2} \text{mom}_{T^2}^2 \prod_{i \notin T^2} x_i \quad (3.5)$$

respectively. They are homogeneous functions of \mathbf{x} of degree L and $L + 1$, respectively. In the second formula, $\text{mom}_{T^2}^2$ defines the squared sum of momenta entering one of the connectivity components of the two-tree [38]. In the present case, these are reduced to first-order polynomials in m such that F is given by the polynomial of the form

$$F(\mathbf{x}; m) = \sum_{i=1}^M c_i x_1^{r_1} \dots x_N^{r_N} m^{2r_{N+1}}, \quad (3.6)$$

with positive expansion coefficients c_i and $r_i \in \{0, 1\}$. The same-sign nature of the c_i 's is the stipulation we alluded to earlier for the successful application of the geometric approach that we are turning to in the next paragraph. The same formula holds for U except for a different set of integers $r_i \in \{0, 1\}$ ($i = 1, \dots, N$) and with $r_{N+1} = 0$,

$$U(\mathbf{x}) = \sum_{i=1}^{\bar{M}} x_1^{r_1} \dots x_N^{r_N}, \quad (3.7)$$

So the Symanzik polynomials correspond to a set of M points $\mathbf{r} = (r_1, \dots, r_N, r_{N+1})$ and \bar{M} points $\bar{\mathbf{r}} = (r_1, \dots, r_N, 0)$ in the $(N + 1)$ -dimensional vector space, respectively. However, the above homogeneity requirements further confine these points to the N -dimensional hyperplane $\sum_{i=1}^N r_i = L + 1$ for F and $(N - 1)$ -dimensional hyperplane $\{\sum_{i=1}^N r_i = L, r_{N+1} = 0\}$ for U .

So in the Feynman parameter space, different scalings of the loop momenta in the small external parameter m are traded for certain equivalent scalings of the integration variables \mathbf{x} . We substitute

$$\mathbf{x} \rightarrow m^{2\mathbf{v}} \mathbf{x}, \quad (3.8)$$

with a $(N + 1)$ -dimensional vector \mathbf{v} of integers, into Eq. (3.1) with (3.4) and after factoring the minimal powers of m from the Symanzik polynomials

$$F(m^{2\mathbf{v}} \mathbf{x}; m) = m^{2\min(\mathbf{v}\cdot\mathbf{r})} F_m(\mathbf{x}), \quad U(m^{2\mathbf{v}} \mathbf{x}) = m^{2\min(\mathbf{v}\cdot\bar{\mathbf{r}})} U_m(\mathbf{x}), \quad (3.9)$$

the residual functions F_m and U_m admit a regular Taylor expansion in m . Then the leading asymptotic contribution to the integral in question is determined by the first term in their Taylor expansion, i.e.,

$$F(m^{2\mathbf{v}} \mathbf{x}; m) \rightarrow m^{2\min(\mathbf{v}\cdot\mathbf{r})} F_0(\mathbf{x}), \quad U(m^{2\mathbf{v}} \mathbf{x}) \rightarrow m^{2\min(\mathbf{v}\cdot\bar{\mathbf{r}})} U_0(\mathbf{x}). \quad (3.10)$$

In this manner, the integral is reduced to an overall ε -dependent power of m accompanied by a coefficient given by an m -independent integral of the residual Symanzik polynomials $U_0(\mathbf{x})$ and $F_0(\mathbf{x})$.

How does one systematically choose the sought-after region vectors \mathbf{v} ? An ingenious recipe was suggested in Ref. [35]. To start with, in order to avoid dealing with two independent polynomials, consider the product

$$F(\mathbf{x}; m)U(\mathbf{x}) = \sum_{i=1}^M c_i x_1^{r_1} \dots x_N^{r_N} m^{2r_{N+1}}, \quad (3.11)$$

with some constants c_i (different from those for the individual Symanzik polynomial $F(\mathbf{x}; m)$) as well as the first N components of the $(N + 1)$ -dimensional vectors $\mathbf{r} = (r_1, \dots, r_N, r_{N+1})$ now drawing values from a larger set $r_i \in \{0, 1, 2\}$. These vectors define the vertices of a convex hull

$$\text{Newt}[UF] = \left\{ \sum_{i=1}^M \alpha_i \mathbf{r}_i : \alpha_i \geq 0 \ \& \ \sum_{i=1}^M \alpha_i = 1 \right\}. \quad (3.12)$$

This is the famed Newton polytope. Its co-dimension one faces are known as facets F and their intersection provides a complementary definition of $\text{Newt}[UF]$. Let's construct all inward-pointing normal vectors \mathbf{v}_f to F . A subset of these with a positive $(N + 1)$ -st component is a set of lower facets F_+ . The region vectors \mathbf{v} are identified by \mathbf{v}_f with $f \in F_+$. This construction was implemented in the automatic code `asy.m` [35, 39], which is currently an integral part of FIESTA5 [40].

3.2 One-loop: MofR and pinching

Coming back to the Sudakov form factor, let us begin with the one-loop integral T_{11} . Assigning the Feynman parameters to the scalar propagators as they appear in the integrand from left to right, the 4-dimensional Newton polytope possesses four lower facets with the following region vectors⁴

$$\mathbf{v}_h = (0, 0, 0), \quad \mathbf{v}_{c1} = (0, 0, 1), \quad \mathbf{v}_{c2} = (0, 1, 0), \quad \mathbf{v}_{us} = (0, 1, 1). \quad (3.13)$$

The corresponding Feynman integrals and their solutions are

$$\begin{aligned} T_{11}^h &= e^{\varepsilon\gamma_E} \mu^{2\varepsilon} \Gamma(1 + \varepsilon) \int d^3\mathbf{x} (x_1 + x_2 + x_3)^{-1+2\varepsilon} (x_2 x_3)^{-1-\varepsilon} \\ &= e^{\varepsilon\gamma_E} \mu^{2\varepsilon} \frac{\Gamma^2(-\varepsilon)\Gamma(1 + \varepsilon)}{\Gamma(1 - 2\varepsilon)}, \end{aligned} \quad (3.14)$$

$$\begin{aligned} T_{11}^{c1} &= e^{\varepsilon\gamma_E} \mu^{2\varepsilon} \Gamma(1 + \varepsilon) \int d^3\mathbf{x} (x_1 + x_2)^{-1+2\varepsilon} (x_1 x_2 + x_2 x_3)^{-1-\varepsilon} \\ &= e^{\varepsilon\gamma_E} \left(\frac{\mu^2}{m^2}\right)^\varepsilon \frac{\Gamma^2(-\varepsilon)\Gamma(\varepsilon)}{2\Gamma(-2\varepsilon)}, \end{aligned} \quad (3.15)$$

$$\begin{aligned} T_{11}^{c2} &= e^{\varepsilon\gamma_E} \mu^{2\varepsilon} \Gamma(1 + \varepsilon) \int d^3\mathbf{x} (x_1 + x_3)^{-1+2\varepsilon} (x_1 x_3 + x_2 x_3)^{-1-\varepsilon} \\ &= e^{\varepsilon\gamma_E} \left(\frac{\mu^2}{m^2}\right)^\varepsilon \frac{\Gamma^2(-\varepsilon)\Gamma(\varepsilon)}{2\Gamma(-2\varepsilon)}, \end{aligned} \quad (3.16)$$

$$\begin{aligned} T_{11}^{us} &= e^{\varepsilon\gamma_E} \mu^{2\varepsilon} \Gamma(1 + \varepsilon) \int d^3\mathbf{x} x_1^{-1+2\varepsilon} (x_1 x_2 + x_2 x_3 + x_3 x_1)^{-1-\varepsilon} \\ &= e^{\varepsilon\gamma_E} \left(\frac{\mu^2}{m^4}\right)^\varepsilon \Gamma(1 - \varepsilon)\Gamma(\varepsilon)^2. \end{aligned} \quad (3.17)$$

Our next order of business is to figure out the reason behind the labeling we attributed to different regions. A naked-eye inspection demonstrates that the dependence on the soft scale m is different for the three groups. The region vector \mathbf{v}_h does not yield any, while it gets singular (for $\varepsilon > 0$) as we move to \mathbf{v}_{ci} becoming the strongest for \mathbf{v}_{us} .

Let us extract the reduced graph of pinch regions for the T_{11} integral from the above MofR consideration. To do it in a way that connects our analysis to traditional pinch-surface analyses, let us do it in the momentum space for the loop momentum k . As exhibited by the components of the region vectors, the scaling of the Feynman parameters translates directly into the inverse scaling of the respective propagators

$$x_i \sim m^{2v_i} \quad \rightarrow \quad D_i^{-2v_i+n_i}, \quad (3.18)$$

up to an arbitrary additive overall shift $\mathbf{n} = (n, \dots, n, 0)$ with $n \in \mathbb{Z}_+$. So that shifting components in each region by an integer to get proper scaling of the loop momentum with

⁴Here and below, we do not display the unit component along the m axis.

external scales

$$\begin{aligned}
\mathbf{v}_h &= (0, 0, 0) : & k^2 &\sim m^0, & (k - P_1)^2 &\sim m^0, & (k + P_2)^2 &\sim m^0, \\
\mathbf{v}_{c1} &= (-1, -1, 0) : & k^2 &\sim m^2, & (k - P_1)^2 &\sim m^2, & (k + P_2)^2 &\sim m^0, \\
\mathbf{v}_{c2} &= (-1, 0, -1) : & k^2 &\sim m^2, & (k - P_1)^2 &\sim m^0, & (k + P_2)^2 &\sim m^2, \\
\mathbf{v}_{us} &= (-2, -1, -1) : & k^2 &\sim m^4, & (k - P_1)^2 &\sim m^2, & (k + P_2)^2 &\sim m^2,
\end{aligned} \tag{3.19}$$

we conclude that \mathbf{v}_h , \mathbf{v}_{c1} , \mathbf{v}_{c2} and \mathbf{v}_{us} correspond to the hard⁵, $k \sim 1$; P_1 -collinear, $k \sim P_1$; P_2 -collinear, $k \sim P_2$ and ultrasoft, i.e., $k \sim m^2$, regions, respectively. So we have three singular pinch surfaces for the one-loop integral: the two collinear regions, and the ultrasoft. As can be easily verified, they are given by the following loop-momentum integrals extended over the entire Minkowski domain

$$T_{11}^{c1} = - \int_k D(k) D(k - P_1) D_{\text{eik}}(k + P_2), \tag{3.20}$$

$$T_{11}^{c2} = - \int_k D(k) D_{\text{eik}}(k - P_1) D(k + P_2), \tag{3.21}$$

$$T_{11}^{\text{us}} = - \int_k D(k) D_{\text{us}}(k - P_1) D_{\text{us}}(k + P_2), \tag{3.22}$$

where we introduced notations for the eikonal and ultrasoft propagators

$$D_{\text{eik}}(k_i \pm P_j) \equiv [\pm 2k_i \cdot p_j]^{-1}, \quad D_{\text{us}}(k_i \pm p_j) \equiv [P_j^2 \pm 2k_i \cdot p_j]^{-1}. \tag{3.23}$$

Here we employed the Sudakov decomposition of the external off-shell momenta

$$P_{1,2} \equiv p_{1,2} + \alpha_i p_{2,1} + p_{1,2}^\perp \tag{3.24}$$

in terms of a pair of light-like vectors p_i ($i = 1, 2$),

$$p_i^2 = 0, \quad p_i \cdot p_i^\perp = 0, \quad p_1 \cdot p_2 = -\frac{1}{2}, \tag{3.25}$$

such that P_i 's are predominantly directed along their low-case counterparts p_i 's.

The above integrals elucidate the underlying physical picture of the process. Namely, the two collinear regions describe the propagation of two energetic scalar jets with almost the speed of light. As a result, each one cannot resolve the internal content of the other due to the Lorentz contraction and thus sees only its overall direction and color, but not more field-specific characteristics like spin. This is encoded in the eikonal form of the interaction. These jets can in turn interact with each other only through the ultrasoft gluon exchange, so as not to change the direction of their propagation. This is again encoded in the eikonal-like interactions but they also accommodate for the non-vanishing virtuality of external lines. This is nothing else than the classical Coleman-Norton interpretation [8] reflecting the pinch

⁵Recall that we have set the hard scale to one, $Q = 1$, to deal with just one dimensionless parameter m in the problem. Otherwise, $k \sim Q$.

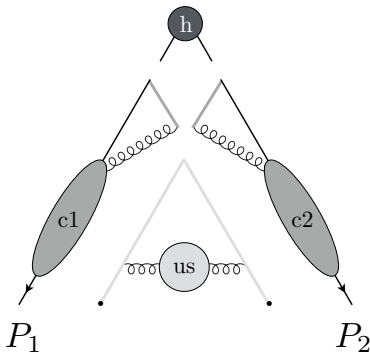


Figure 2. Leading pinch regions of the one-loop integral T_{11} for the off-shell Sudakov form factor. The lighter the blob the softer are the loop momenta circulating in quantum loops.

surfaces in the near mass-shell limit. Obviously, the hard region does not possess mass singularities as it is m -independent and is determined by the integral

$$T_{11}^h = - \int_k D_0(k) D_0(k - P_1) D_0(k + P_2), \quad (3.26)$$

with massless, i.e., on-shell external line, propagators $D_0(k \pm P_i) = D(k \pm p_i)$.

To conclude, the one-loop analysis gives us the following asymptotic form of the one-loop graph as $m \rightarrow 0$

$$T_{11} = T_{11}^h + T_{11}^{c1} + T_{11}^{c2} + T_{11}^{us}, \quad (3.27)$$

with the corresponding reduced one-loop graph on the leading pinch surface is shown in Fig. 2. Let us point out that from the momentum-space perspective, an analogous one-loop analysis was performed in Ref. [41].

4 Jet function: definition and one-loop result

Having established the form of integrals for incoherent momentum components defining the pinched Sudakov form factor at one loop, we are now in a position to find their operator content. The advantage of the MofR compared to more traditional methods based on Landau equations is that it provides us with a precise form of integrands valid over the entire Minkowski space: there is no need to assume any momentum cut-offs.

We first turn to the collinear regions. Since both of them are identical up to the exchange of the legs' labels, it suffices to discuss just one. With external scalar lines being off the mass-shell, this requires an interpretation for the states $|P_1, P_2\rangle_{\text{amp}} = |P_1\rangle_{\text{amp}} \otimes |P_2\rangle_{\text{amp}}$. We understand them as

$$|P_i\rangle_{\text{amp}} \equiv \tilde{\phi}^\dagger(P_i)|0\rangle_{\text{amp}} = \tilde{\phi}^\dagger(P_i)|0\rangle [iD(P_i)]^{-1}, \quad (4.1)$$

where $\tilde{\phi}^\dagger$ is the Fourier transform of the scalar field ϕ^\dagger in the Heisenberg representation. Now, since the interaction of this leg with the one in the opposite jet is eikonal, this implies that the latter can be replaced by a Wilson line stretching from the source to infinity along the light-like direction p_i . Thus we can immediately borrow the well-known definition of the jet function from the on-shell case [14] and define

$$J_1 \equiv \langle 0 | [\infty, 0]_{p_2} \phi(0) | P_1 \rangle_{\text{amp}}, \quad (4.2)$$

where we introduced the light-like Wilson line

$$[\infty, 0]_p \equiv P \exp \left(i g_{\text{YM}} \int_0^\infty d\tau p \cdot A(\tau p) \right). \quad (4.3)$$

There exists a potential subtlety due to the overcounting of the ultrasoft region from the off-shell leg in this definition. As in the on-shell approach, it can be eliminated by introducing the concept of the eikonal jet [12], i.e., when the scalar line itself is replaced by the Wilson line. Within the framework of effective field theories, these are known as zero-bin subtractions [11, 42]. For our observable, the external leg is off the mass-shell and thus its treatment needs care. It will be performed in the next section. The upshot is that the eikonal jet gets replaced for the case at hand by the ultrasoft jet function given by the vacuum expectation value of the operator

$$J_1^{\text{us}} \equiv \int_0^\infty d\sigma e^{i\sigma P_1^2} \langle 0 | [\infty, 0]_{p_2} [2p_1\sigma, 0]^\dagger | 0 \rangle_{\text{amp}}. \quad (4.4)$$

The double counting is then removed by means of the substitution

$$J_1 \rightarrow J_1 / J_1^{\text{us}}. \quad (4.5)$$

The same holds for the other jet upon the interchange of the labels $1 \leftrightarrow 2$. Notice, however, since MofR universally employs dimensional regularization to tame singularities, the ultrasoft jet function is given by scaleless integrals at each order of perturbation theory and is thus set to one, $J_{\text{dimreg}}^{\text{us}} = 1$. It is a well-known fact in the effective theories as well [32].

A one-loop calculation in the Feynman gauge then gives for the off-shell jet function (4.2),

$$\begin{aligned} J_1 &= 1 + i g^2 \int_k \int_0^\infty d\sigma e^{i\sigma(p_1 \cdot k)} p_1 \cdot (2P_2 - k) D(k) D(k - P_2) + O(g^4) \\ &= 1 - g^2 e^{\varepsilon\gamma_E} \left(\frac{\mu^2}{m^2} \right)^\varepsilon \frac{\Gamma^2(-\varepsilon)\Gamma(\varepsilon)}{2\Gamma(-2\varepsilon)} + O(g^4), \end{aligned} \quad (4.6)$$

and demonstrates the equivalence to MofR's $T_{11}^{\text{c}1}$. A two-loop calculation of this jet factor will be performed elsewhere.

As a next step, let us focus on the consideration of the near mass-shell limit of the scalar Green function which was instrumental for the proper definition of the ultrasoft jet function introduced above. Along the way, we will uncover the form for an operator defining the ultrasoft region of the pinched Sudakov form factor as well.

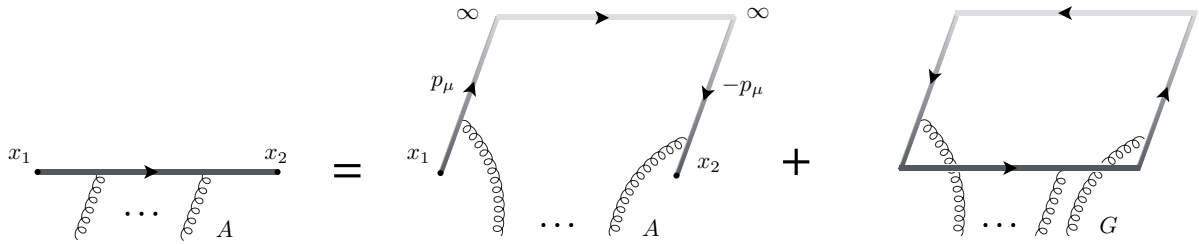


Figure 3. Leading singularity of the gauge-field propagator in the external field and contour deformation.

5 Ultrasoft function

Let us now discuss the ultrasoft function. It involves propagators in the near mass-shell limit. So we start our analysis by considering their infrared properties.

5.1 Definition

To analyze the infrared singularities of the scalar propagator, we will use a variant of the background field method [43]. It will echo the classical analysis of the infrared asymptotics of the electron Green function in QED [44].

As was suggested by the analysis in the previous sections, ultrasoft singularities in Green functions stem from modes of very long wavelength. Thus, let us separate quantum gauge fields in terms of a sum of the fast a and slow A fields without specifying the precise location of the interface since it will not be relevant at the end, $A \rightarrow a + A$. Then, according to the analysis in the Appendix A, the scalar propagator in the external field A is given by the product

$$D_A(x_2, x_1) = D_0(x_2 - x_1)[x_2, x_1], \quad (5.1)$$

where the slow modes enter only through the Wilson line along a straight segment connecting the points x_1 and x_2

$$[x_2, x_1] \equiv P \exp \left(i g_{\text{YM}} \int_{x_1}^{x_2} dx \cdot A \right), \quad (5.2)$$

and the hard field was integrated out. Without affecting the leading light-cone singularity of the scalar propagator, the integration contour entering the Wilson segment can be deformed to any other smooth shape since the difference is power-suppressed⁶. For instance, as we demonstrated in Fig. 3, we can re-write $[x_2, x_1]$ identically as a difference between the staple-like contour and a closed loop. The gluons emitted by the closed loop are twist-one by default

⁶See Ref. [45] for a study relating anomalous dimension for various Wilson loop contours in the light-like case.

since they are expressible in terms of the gluon field strength tensor. Thus they yield power-suppressed contributions in the light-cone kinematics. Thus, up to power corrections the straight contour is given the staple⁷,

$$[x_2, x_1] = [\infty, x_2]_v^\dagger [\infty, x_1]_v (1 + O(G_{\mu\nu})), \quad (5.3)$$

where the two rays are pointing along an arbitrary direction v_μ . In particular, if $x_1 = 0$ and x_2 is changing along a the same fixed vector $x_2 = \tau v$, $[\infty, x_2]_v^\dagger [\infty, x_1]_v$ collapses on this line $[\tau v, 0]_v$.

For identification of the operator content of Eq. (3.22), we need the Fourier transform of the scalar propagator. It reads

$$iD_A(P) = \int d^D x e^{iP \cdot x} D_0(x)[x, 0] = \int_0^\infty d\sigma \int \frac{d^D k}{(2\pi)^D} e^{i\sigma(P+k)^2} \widetilde{W}[k], \quad (5.4)$$

here we used the Schwinger representation of the bare propagator $D(P+k)$ and the Fourier image of the Wilson segment

$$\widetilde{W}[k] \equiv \int d^D x e^{ix \cdot k} [x, 0].$$

So far all of the transformations were exact. Now, for gluons connecting to the Wilson line in the ultrasoft region, i.e., $|P^2| \gg |k^2|$, we can expand the Lorentz-invariant exponent as $(P+k)^2 \simeq P^2 + 2k \cdot p$ with light-like p , and perform the inverse Fourier transformation of $\widetilde{W}[k]$ back to the coordinate space. Finally, we deduce

$$D_A(P) = \int_0^\infty d\sigma e^{i\sigma P^2} [2\sigma p, 0]_p, \quad (5.5)$$

where we chose the link to be along p . As we can see from here, the nonzero virtuality of the scalar propagator introduces a segment Wilson line along the light-like direction p_μ and its finite extent is inversely proportional to the virtuality P^2 .

Using Eq. (5.5), we can immediately determine the operator definition of the ultrasoft factor,

$$W(P_1, P_2) = \int_0^\infty d\sigma_1 d\sigma_2 e^{i\sigma_1 P_1^2 + i\sigma_2 P_2^2} \mathcal{W}(\sigma_1, \sigma_2), \quad (5.6)$$

with the integrand being

$$\mathcal{W}(\sigma_1, \sigma_2) \equiv \langle 0 | [2\sigma_1 p_1, 0] [2\sigma_2 p_2, 0]^\dagger | 0 \rangle. \quad (5.7)$$

Everywhere here and below it is tacitly implied that P_i^2 acquires a small positive imaginary part $P_i^2 + i0_+$ for convergence of the integrals in Eq. (5.6). This quantity coincides with the

⁷The top of the staple can be ignored in all covariant gauges, but not in the light-like and axial types due to zero modes which can propagate infinite distances, see, e.g., [46].

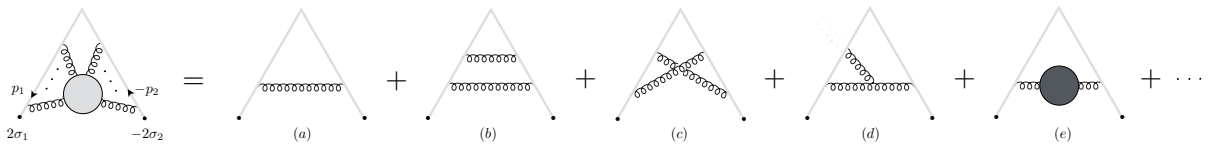


Figure 4. Graphs contributing to the one- (a) and two-loop ($b - e$) integrands \mathcal{W} of the ultrasoft factor W . A mirror image graph to (d) is not shown.

so-called IR factor introduced several decades ago in Refs. [5, 47]. But this is it as far as our agreement goes. Our conclusions regarding its renormalization properties will differ.

Obviously, as it stands, the above vacuum expectation value (5.7), being defined by Wilson lines on finite intervals, is not gauge invariant: even a small gauge transformation of the gluon field will induce nonvanishing gauge matrices at its ends. However, we are not actually after the ultrasoft function $W(P_1, P_2)$ for finite virtualities but rather only for their asymptotically small values, i.e., on the pinch surface $P_i^2 \rightarrow 0$. The saddle-point approximation for (5.6) then implies that σ_i 's tend to infinity and, in this fashion, the integrand \mathcal{W} of the ultrasoft function restores its gauge invariance. From the momentum-space perspective, this indicates that we are interested only in contributions at the poles $P_i^2 = 0$. Thus, it makes sense in what follows to introduce an amputated ultrasoft function S as a pole part of W

$$W(P_1, P_2) \equiv [iD(P_1)]S(P_1, P_2)[iD(P_2)] + \text{less singular terms}, \quad (5.8)$$

with the scalar propagators $D(P_i) = [P_i^2]^{-1}$, where, as alluded to earlier, we do not exhibit the imaginary shift. The residual dependence of the left-hand side on P_i^2 is not rational and, as we will see below, is in fact non-analytic in these virtualities.

5.2 Perturbative expansion: One loop

The ultrasoft function W develops perturbative expansion in g . We will now calculate them order by order in the Feynman gauge. The light-like nature of the segments eliminates self-contractions of gluons from each of them individually. So we need to address only diagrams where the left link is connected to the right one. Up to two-loop order, its integrand receives contributions from Feynman diagrams shown in Fig. 4.

We start from the first quantum correction displayed in Fig. 4 (a). The integrand of the ultrasoft function reads

$$\mathcal{W}_{(a)}^{(1)} = g_{\text{YM}}^2 \int_0^{2\sigma_1} d\tau_1 \int_{-2\sigma_2}^0 d\tau_2 \langle A_+(p_1\tau_1)A_-(-p_2\tau_2) \rangle_0, \quad (5.9)$$

where $A_+ \equiv p_1 \cdot A$ and $A_- \equiv p_2 \cdot A$. Here $\langle \dots \rangle_0$ stands for the vacuum expectation value in the interaction picture. Making use of the definition for the gluon propagator in the Feynman gauge

$$\langle A_\mu^a(x_1)A_\nu^b(x_2) \rangle_0 \equiv -i\delta^{ab}g_{\mu\nu}D(x_1 - x_2), \quad (5.10)$$

and performing the half-range Fourier transform, its one-loop momentum-space integral representation becomes for the amputated function (5.8)

$$S_{(a)}^{(1)} = 2g^2 \int_k D(k) D_{\text{us}}(k - p_1) D_{\text{us}}(k + p_2). \quad (5.11)$$

It is written in terms of the momentum-space gluon propagator (denoted by the same letter as the coordinate one)

$$D(x) \equiv \int \frac{d^D k}{(2\pi)^D} e^{-ix \cdot k} D(k), \quad (5.12)$$

as well as the ultrasoft ones (3.23). The calculation of the resulting momentum integral is straightforward and we find for it

$$S_{(a)}^{(1)} = -2g^2 w_{(a)}, \quad (5.13)$$

where

$$w_{(a)} = e^{\varepsilon \gamma_E} \left(\frac{\mu^2}{m^4} \right)^\varepsilon \Gamma^2(\varepsilon) \Gamma(1 - \varepsilon). \quad (5.14)$$

5.3 Two loops

Let us now move on to the calculation of contributing two-loop graphs.

5.3.1 Ladder graphs

At two loops, we start with the iterated (planar and non-planar) ladders. Expanding each path-ordered exponents to $O(g^2)$, the integrals defining these contributions read

$$\mathcal{W}_{(b+c)}^{(2)} = g_{\text{YM}}^4 \int_0^{2\sigma_1} d\tau_1 \int_0^{\tau_1} d\tau'_1 \int_{-2\sigma_2}^0 d\tau_2 \int_{-2\sigma_2}^{\tau_2} d\tau'_2 \langle A_+(p_1 \tau_1) A_+(p_1 \tau'_1) A_-(-p_2 \tau_2) A_-(-p_2 \tau'_2) \rangle_0. \quad (5.15)$$

Wick contraction yields then planar and nonplanar double ladders

$$\begin{aligned} \langle A_+(p_1 \tau_1) A_+(p_1 \tau'_1) A_-(-p_2 \tau_2) A_-(-p_2 \tau'_2) \rangle_0 &= \frac{1}{4} N_c^2 \\ &\times \left[D(p_1 \tau_1 + p_2 \tau'_2) D(p_1 \tau'_1 + p_2 \tau_2) + \frac{1}{2} D(p_1 \tau_1 + p_2 \tau_2) D(p_1 \tau'_1 + p_2 \tau'_2) \right]. \end{aligned} \quad (5.16)$$

As it is obvious from the double-line representation (see Fig. 5), the nonplanar contribution is nevertheless of the leading color. Performing the half-range Fourier transformation, we find

$$S_{(b+c)}^{(2)} = 4g^4 \left[w_{(b)} + \frac{1}{2} w_{(c)} \right], \quad (5.17)$$

with

$$w_{(b)} = \int_{k_1, k_2} D(k_1) D(k_2) D_{\text{us}}(k_1 - p_1) D_{\text{us}}(k_1 + k_2 - p_1) D_{\text{us}}(k_1 + p_2) D_{\text{us}}(k_1 + k_2 + p_2)$$

$$= e^{2\varepsilon\gamma_E} \left(\frac{\mu^2}{m^4} \right)^{2\varepsilon} \Gamma^2(-\varepsilon)\Gamma^2(2\varepsilon), \quad (5.18)$$

$$w_{(c)} = \int_{k_1, k_2} D(k_1)D(k_2)D_{\text{us}}(k_1 - p_1)D_{\text{us}}(k_1 + k_2 - p_1)D_{\text{us}}(k_2 + p_2)D_{\text{us}}(k_1 + k_2 + p_2)$$

$$= e^{2\varepsilon\gamma_E} \left(\frac{\mu^2}{m^4} \right)^{2\varepsilon} \Gamma^2(-\varepsilon)\Gamma^2(2\varepsilon). \quad (5.19)$$

Both of them are given by identical expressions.

Notice that we have not used the non-Abelian exponentiation theorem in our treatment of iterated ladders. The reason being that one has to perform the half-line Fourier transform at the end of the calculation which requires expanding the exponentiated contribution in the perturbative series anyway.

5.3.2 Non-Abelian graphs

The contribution from the non-Abelian graph in Fig. 4 (d) to the integrand is

$$\mathcal{W}_{(d)}^{(2)} = g_{\text{YM}}^4 \int_0^{2\sigma_1} d\tau_1 \int_0^{\tau_1} d\tau'_1 \int_{-2\sigma_2}^0 d\tau_2 \int d^D x_0 \langle A_+(2p_1\tau_1)A_+(2p_1\tau'_1)A_-(-2p_2\tau_2)V_g(x_0) \rangle_0, \quad (5.20)$$

where out of three terms of the momentum-space Feynman rule for the three-gluon vertex $V_g = f^{abc}(\partial_\mu A_\nu^a)A_\mu^b A_\nu^c$ only two contribute non-trivially giving

$$\mathcal{W}_{(d)}^{(2)} = \frac{i}{4}g^4 \int_0^{2\sigma_1} d\tau_1 \int_0^{\tau_1} d\tau'_1 \int_{-2\sigma_2}^0 d\tau_2$$

$$\times \int_{k_1, k_2} e^{-ip_1 \cdot (\tau_1 k_1 + \tau'_1 k_2) + i\tau_2 p_2 \cdot (k_1 + k_2)} p_1 \cdot (k_2 - k_1) D(k_1)D(k_2)D(k_1 + k_2). \quad (5.21)$$

Let us describe the next couple of steps in more detail since this will exhibit the gauge-restoring limit we advocated at the end of Sect. 5.1. Namely, performing the nested line integrals, we find

$$\mathcal{W}_{(d)}^{(2)} = \frac{i}{4}g^4 \int_{k_1, k_2} D(k_1)D(k_2)D(k_1 + k_2)E_{\sigma_2}(0; p_2 \cdot (k_1 + k_2))$$

$$\times [E_{\sigma_1}(0; p_1 \cdot k_1) - 2E_{\sigma_1}(0; p_1 \cdot (k_1 + k_2)) + E_{\sigma_1}(p_1 \cdot k_1; p_1 \cdot (k_1 + k_2))]. \quad (5.22)$$

where we used the notation for the function

$$E_\sigma(r_1; r_2) \equiv \frac{e^{-2i\sigma r_1} - e^{-2i\sigma r_2}}{r_1 - r_2}. \quad (5.23)$$

In the infinite-segment limit, the first two terms in the square brackets generate nonvanishing contributions, while the last one vanishes due to the near-total cancellation of rapid oscillations. This can also be verified by performing the half-range Fourier transforms and noticing

that this term does not induce a pole in P_1^2 . Neglecting it, we then find the contribution to the amputated ultrasoft function

$$S_{(d)}^{(2)} = g^4 w_{(d)}, \quad (5.24)$$

with two-loop integral evaluated to

$$\begin{aligned} w_{(d)} &= \int_{k_1, k_2} D(k_1) D(k_2) D(k_1 + k_2) D_{\text{us}}(k_1 + k_2 + p_2) [2D_{\text{us}}(k_1 + k_2 - p_1) - D_{\text{us}}(k_1 - p_1)] \\ &= 2 e^{2\varepsilon\gamma_E} \left(\frac{\mu^2}{m^4}\right)^{2\varepsilon} \Gamma(-\varepsilon)\Gamma(2\varepsilon) [\Gamma(-2\varepsilon)\Gamma(2\varepsilon)\Gamma(1 + \varepsilon) - \Gamma(1 - \varepsilon)\Gamma(-1 + 2\varepsilon)]. \end{aligned} \quad (5.25)$$

Notice that the second term in the square bracket does not possess uniform transcendentality (UT) when expanded in ε . However, it has a bubble subgraph as its inner loop and it will be canceled, after doubling this contribution thanks to the mirror non-Abelian image to Fig. 4 (d), by the vacuum polarization diagram that we finally turn to next.

5.3.3 Self-energy graphs

The two-loop self-energy diagram in Fig. 4 (e) is the only one at this loop order that explicitly depends on the number of gluon polarization circulating in the loop, i.e., it displays full-fledged scheme dependence. To preserve supersymmetry we have to choose Siegel's dimensional reduction [26] as opposed to the conventional dimensional regularization. To this end, we can borrow the result from Ref. [48], where the one-loop effect from the $\mathcal{N} = 4$ fields on the gluon propagator was calculated to all orders in ε . Thus, we just need to substitute the gluon propagator $D(k)$ in Eq. (5.11) with

$$D(k) \rightarrow -2g^2 \left(\frac{\mu^2}{-k^2}\right)^\varepsilon e^{\varepsilon\gamma_E} \frac{\Gamma(\varepsilon)\Gamma^2(1 - \varepsilon)}{\Gamma(2 - 2\varepsilon)}. \quad (5.26)$$

The calculation of the remaining k -integrals gives for the amputated ultrasoft function

$$S_{(e)}^{(2)} = g^4 w_{(e)}, \quad (5.27)$$

with

$$w_{(e)} = -2 \left(\frac{\mu^2}{m^4}\right)^{2\varepsilon} e^{2\varepsilon\gamma_E} \frac{\Gamma(\varepsilon)\Gamma^2(1 - \varepsilon)}{\Gamma(2 - 2\varepsilon)} \frac{\Gamma(1 - 2\varepsilon)\Gamma^2(2\varepsilon)}{\Gamma(1 + \varepsilon)}. \quad (5.28)$$

Elementary simplifications then demonstrate that indeed this is twice the UT-violating contribution from the non-Abelian diagram. Thus this cancellation enforces the well-known UT feature of the maximally supersymmetric theory exhibited here through the ultrasoft function.

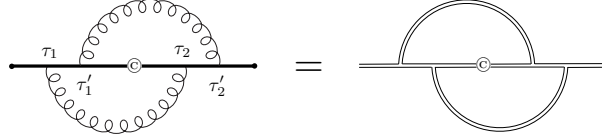


Figure 5. A double line representation for the nonplanar ladder in Fig. 4 (c). The vertex \textcircled{C} stands for the location of the cusp.

5.3.4 The sum

Before we take the sum of all the graphs, we need to take care of the overall ultraviolet subtraction of the segmented Wilson line. However, the only one that would be needed for its infinite- σ limit is the gauge invariant counterterm due to the coupling renormalization, i.e., proportional to the one-loop beta-function. The latter vanishes, however, and thus there are no further contributions to account for. Adding all of the above diagrams gives us the final expression

$$S = 1 + g^2[-2T_{11}^{\text{us}}] + g^4[4T_{21}^{\text{us}} + T_{22}^{\text{us}}] + O(g^6), \quad (5.29)$$

with

$$T_{11}^{\text{us}} = \left(\frac{\mu^2}{m^4}\right)^\varepsilon e^{\varepsilon\gamma_E} \Gamma^2(\varepsilon)\Gamma(1-\varepsilon), \quad (5.30)$$

$$T_{21}^{\text{us}} = \left(\frac{\mu^2}{m^4}\right)^{2\varepsilon} e^{2\varepsilon\gamma_E} \Gamma^2(2\varepsilon)\Gamma^2(-\varepsilon), \quad (5.31)$$

$$T_{22}^{\text{us}} = 2 \left(\frac{\mu^2}{m^4}\right)^{2\varepsilon} e^{2\varepsilon\gamma_E} \Gamma^2(2\varepsilon)\Gamma(-\varepsilon)[\Gamma(-\varepsilon) - \Gamma(1-2\varepsilon)\Gamma(\varepsilon)], \quad (5.32)$$

where we intentionally wrote it in a form that resembles the scalar integral expansion of the two-loop form factor. In this manner, it will be easier for us to compare these expressions with the results of MofR to be performed in the following section. In fact, ultrasoft function exponentiates including the finite terms and reads

$$\log S = -g^2 \left(\frac{\mu^2}{m^4}\right)^\varepsilon \left(\frac{2}{\varepsilon^2} + 3\zeta_2\right) + g^4 \left(\frac{\mu^2}{m^4}\right)^{2\varepsilon} \left(\frac{5\zeta_2}{\varepsilon^2} - \frac{7\zeta_3}{\varepsilon} + 71\zeta_4\right) + \dots, \quad (5.33)$$

with the exponent possessing at most order ε^{-2} poles to this order in coupling. This behavior persists to all orders in 't Hooft coupling according to the conjecture we put forward in Ref. [1].

6 All-order factorization: a proposal

With perturbative results obtained so far, we can now propose a naive factorization formula for the off-shell Sudakov form factor. Namely, restoring the ultrasoft jet factors, anticipating

a potential use of regularizations different from dimensional, we write for the near mass-shell limit as

$$\mathcal{F}_2^{\text{naive}} = H(\mu^2, \varepsilon) \frac{J_1(\mu^2/m^2, \varepsilon)}{J_1^{\text{us}}(\mu^2/m^2, \varepsilon)} \frac{J_2(\mu^2/m^2, \varepsilon)}{J_2^{\text{us}}(\mu^2/m^2, \varepsilon)} S(\mu^2/m^4, \varepsilon), \quad (6.1)$$

where we assumed the same virtuality for both external legs, $P_i^2 = -m^2 \rightarrow 0$. The operator definitions for all pinch surfaces were introduced in Eqs. (4.2), (4.4), (5.8), respectively. H is the hard matching coefficient. If one wishes to restore the dependence on the hard scale Q^2 , the following substitutions are to be made

$$\mu \rightarrow \mu/Q, \quad m \rightarrow m/Q. \quad (6.2)$$

In this manner, one recognizes the two infrared scales involved in the problem, the collinear and the ultrasoft [5, 49, 50]

$$\mu_{\text{col}} = m, \quad \mu_{\text{us}} = m^2/Q. \quad (6.3)$$

Let us now proceed with its two-loop test.

7 Two-loop test

As before, we will rely on MofR to verify the formula (6.1). Since we have a clear identification of the hard, collinear and ultrasoft regions at one loop, which are associated with $\mu^{2\varepsilon}$, $(\mu^2/m^2)^\varepsilon$ and $(\mu^2/m^4)^\varepsilon$ scalings of contributing regions, respectively, it should be straightforward to do the same at two loops. With each loop integration producing each of the above, we anticipate six scalings:

$$\begin{aligned} \text{h-h} : \mu^{4\varepsilon}, & & \text{h-c} : (\mu^4/m^2)^\varepsilon, & & \text{h-us} : (\mu^4/m^4)^\varepsilon, \\ \text{c-c} : (\mu^2/m^2)^{2\varepsilon}, & & \text{c-us} : (\mu^4/m^6)^\varepsilon, & & \text{us-us} : (\mu^2/m^4)^{2\varepsilon}. \end{aligned} \quad (7.1)$$

The total number of regions in each two-loop graph can be up to sixteen via naive counting due to the doubling of the collinear ones, one for each leg, $\#(\text{h}, \text{c1}, \text{c2}, \text{us})^2 = 16$. However, there are far fewer in the iterated ladder since the inner, i.e., k_2 -loop, is always harder than the outer one being closer to the source. In the crossed ladder case, on the other hand, both loop momenta enter symmetrically and all sixteen regions can and do realize. However, as we will see from our analysis, the precise identification of regions will be different from the above naive counting. As we can see the double-collinear and hard-ultrasoft regions possess the same scaling. However, they are easy to disentangle from each other by studying an explicit form of components of the region vectors.

7.1 MofR vs. naive factorization

Our analysis of associated Newton polytopes with `asy` for the two scalar integrals T_{21} and T_{22} , defined by Eqs. (2.4) and (2.5), reveals 9 and 16 lower facets, respectively. We choose

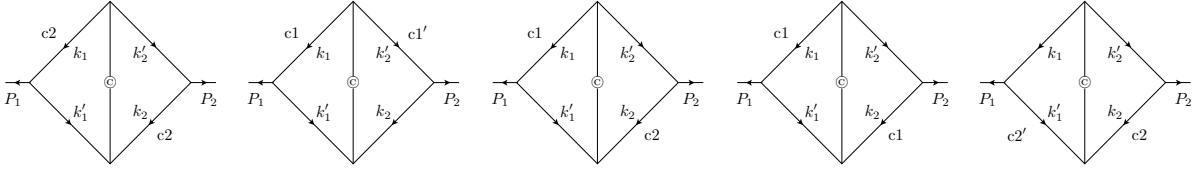


Figure 6. Momentum flow in the non-planar graph and all collinear-collinear regions in it.

to label the regions in the order k_2 - k_1 of the loop integrals reflecting the momentum flow in Fig. 1. They are defined by the normal vectors

$$\begin{aligned}
\mathbf{v}_{h-h} &= (0, 0, 0, 0, 0, 0), & \mathbf{v}_{h-c1} &= (0, 1, 0, 1, 1, 1), & \mathbf{v}_{h-c2} &= (0, 1, 1, 1, 0, 1), \\
\mathbf{v}_{c1-c1} &= (0, 0, 0, 0, 1, 1), & \mathbf{v}_{c2-c2} &= (0, 0, 1, 1, 0, 0), & \mathbf{v}_{h-us} &= (0, 2, 1, 2, 1, 2), \\
\mathbf{v}_{c1-us} &= (0, 1, 1, 1, 1, 2), & \mathbf{v}_{c2-us} &= (0, 1, 1, 2, 1, 1), & \mathbf{v}_{us-us} &= (0, 0, 1, 1, 1, 1),
\end{aligned} \tag{7.2}$$

for T_{21} , and

$$\begin{aligned}
\mathbf{v}_{h-h} &= (0, 0, 0, 0, 0, 0), & \mathbf{v}_{c2-h} &= (1, 0, 1, 1, 0, 1), & \mathbf{v}_{h-c1} &= (0, 1, 0, 1, 1, 1), & \mathbf{v}_{c2-c2} &= (0, 0, 1, 1, 0, 0), \\
\mathbf{v}_{c1'-c1} &= (0, 1, 0, 1, 0, 0), & \mathbf{v}_{c2-c1} &= (0, 0, 0, 1, 0, 1), & \mathbf{v}_{c1-c1} &= (0, 0, 0, 0, 1, 1), & \mathbf{v}_{c2-c2'} &= (1, 0, 0, 0, 0, 1), \\
\mathbf{v}_{us'-c1} &= (1, 1, 1, 2, 0, 1), & \mathbf{v}_{c2-us} &= (0, 1, 1, 2, 1, 1), & \mathbf{v}_{us-c1} &= (1, 0, 1, 1, 1, 2), & \mathbf{v}_{c2-us'} &= (1, 1, 0, 1, 1, 2), \\
\mathbf{v}_{us'-us'} &= (1, 1, 0, 1, 0, 1), & \mathbf{v}_{us-us} &= (0, 0, 1, 1, 1, 1), & \mathbf{v}_{us'-us} &= (0, 1, 1, 2, 0, 0), & \mathbf{v}_{us-us'} &= (1, 0, 0, 0, 1, 2),
\end{aligned} \tag{7.3}$$

for T_{22} . What might be a bit puzzling is the number of collinear-collinear regions in the crossed ladder: there are five instead of the expected four. But a quick look at the momentum flow in the graph, see, Fig. 6, confirms that this number is indeed correct. We also clarify in that figure the nomenclature used in the naming of the region vectors. Since we use non-symmetric routing of the loop momenta in an otherwise symmetric non-planar graph, the regions with primes in the k_2 - k_1 labeling scheme correspond to the shifted momenta $k_2 \rightarrow k_2' = k_2 + p_2$ and $k_1 \rightarrow k_1' = k_1 - p_1$, respectively.

Feynman parameter integrals presented in Appendix B were transformed into the Mellin-Barnes form making use of the Mathematica package `MBcreate.m` [51] and evaluated as a Laurent expansion in ε . We found for these

$$T_{21}^{h-h} = \mu^{4\varepsilon} \left[\frac{1}{4\varepsilon^4} + \frac{5\zeta_2}{4\varepsilon^2} + \frac{29\zeta_3}{6\varepsilon} + \frac{135\zeta_4}{16} + O(\varepsilon) \right] \tag{7.4}$$

$$T_{21}^{h-c1} = T_{21}^{h-c2} = \left(\frac{\mu^4}{m^2} \right)^\varepsilon \left[-\frac{1}{2\varepsilon^4} - \frac{\zeta_2}{\varepsilon^2} - \frac{11\zeta_3}{3\varepsilon} - \frac{21\zeta_4}{2} + O(\varepsilon) \right] \tag{7.5}$$

$$T_{21}^{c1-c1} = T_{21}^{c2-c2} = \left(\frac{\mu^2}{m^2} \right)^{2\varepsilon} \left[\frac{1}{4\varepsilon^4} + \frac{\zeta_2}{4\varepsilon^2} + \frac{5\zeta_3}{6\varepsilon} + \frac{163\zeta_4}{16} + O(\varepsilon) \right], \tag{7.6}$$

$$T_{21}^{h-us} = \left(\frac{\mu^4}{m^4} \right)^\varepsilon \left[\frac{1}{\varepsilon^4} + \frac{\zeta_2}{\varepsilon^2} - \frac{8\zeta_3}{3\varepsilon} - \frac{5\zeta_4}{4} + O(\varepsilon) \right], \tag{7.7}$$

$$T_{21}^{c1-us} = T_{21}^{c2-us} = \left(\frac{\mu^4}{m^6} \right)^\varepsilon \left[-\frac{1}{2\varepsilon^4} - \frac{\zeta_2}{\varepsilon^2} + \frac{7\zeta_3}{3\varepsilon} - 3\zeta_4 + O(\varepsilon) \right], \tag{7.8}$$

$$T_{21}^{\text{us-us}} = \left(\frac{\mu^2}{m^4} \right)^{2\varepsilon} \left[\frac{1}{4\varepsilon^4} + \frac{5\zeta_2}{4\varepsilon^2} - \frac{7\zeta_3}{6\varepsilon} + \frac{159\zeta_4}{16} + O(\varepsilon) \right]. \quad (7.9)$$

and

$$T_{22}^{\text{h-h}} = \mu^{4\varepsilon} \left[\frac{1}{\varepsilon^4} - \frac{6\zeta_2}{\varepsilon^2} - \frac{83\zeta_3}{3\varepsilon} - \frac{177\zeta_4}{4} + O(\varepsilon) \right], \quad (7.10)$$

$$T_{22}^{\text{c2-h}} = T_{22}^{\text{h-c1}} = \left(\frac{\mu^4}{m^2} \right)^\varepsilon \left[-\frac{2}{\varepsilon^4} + \frac{8\zeta_2}{\varepsilon^2} + \frac{100\zeta_3}{3\varepsilon} + 63\zeta_4 + O(\varepsilon) \right], \quad (7.11)$$

$$T_{22}^{\text{c2-c2}} = T_{22}^{\text{c1'-c1}} = T_{22}^{\text{c1-c1}} = T_{22}^{\text{c2-c2'}} = \left(\frac{\mu^2}{m^2} \right)^{2\varepsilon} \left[\frac{1}{2\varepsilon^4} - \frac{\zeta_2}{\varepsilon^2} - \frac{53\zeta_3}{6\varepsilon} - \frac{167\zeta_4}{8} + O(\varepsilon) \right], \quad (7.12)$$

$$T_{22}^{\text{c2-c1}} = \left(\frac{\mu^2}{m^2} \right)^{2\varepsilon} \left[\frac{4}{\varepsilon^4} - \frac{4\zeta_2}{\varepsilon^2} - \frac{56\zeta_3}{3\varepsilon} - 21\zeta_4 + O(\varepsilon) \right], \quad (7.13)$$

$$T_{22}^{\text{us'-c1}} = T_{22}^{\text{c2-us}} = T_{22}^{\text{us-c1}} = T_{22}^{\text{c2-us'}} = \left(\frac{\mu^4}{m^6} \right)^\varepsilon \left[-\frac{1}{\varepsilon^4} - \frac{2\zeta_2}{\varepsilon^2} + \frac{14\zeta_3}{3\varepsilon} - 6\zeta_4 + O(\varepsilon) \right], \quad (7.14)$$

$$T_{22}^{\text{us'-us'}} = T_{22}^{\text{us-us}} = \left(\frac{\mu^2}{m^4} \right)^{2\varepsilon} \left[\frac{1}{4\varepsilon^4} + \frac{5\zeta_2}{4\varepsilon^2} - \frac{7\zeta_3}{6\varepsilon} + \frac{159\zeta_4}{16} + O(\varepsilon) \right], \quad (7.15)$$

$$T_{22}^{\text{us'-us}} = T_{22}^{\text{us-us'}} = \left(\frac{\mu^2}{m^4} \right)^{2\varepsilon} \left[\frac{1}{4\varepsilon^4} + \frac{7\zeta_2}{4\varepsilon^2} - \frac{2\zeta_3}{3\varepsilon} + \frac{295\zeta_4}{16} + O(\varepsilon) \right]. \quad (7.16)$$

With these findings in our hands, we can verify that the sum of double ultrasoft regions coincides with the Laurent expansion of the two-loop expressions T_{21}^{us} and T_{22}^{us} stemming from the Wilson line analysis, i.e., Eqs. (5.31) and (5.32),

$$T_{22}^{\text{us}} = T_{21}^{\text{us-us}} + O(\varepsilon), \quad (7.17)$$

$$T_{22}^{\text{us}} = T_{22}^{\text{us'-us'}} + T_{22}^{\text{us-us}} + T_{22}^{\text{us'-us}} + T_{22}^{\text{us-us'}} + O(\varepsilon). \quad (7.18)$$

Therefore, it seems only natural to identify all double-collinear regions with labels ci , ci' with the jet function J_i ,

$$J_i = 1 + g^2[-2T_{11}^{ci}] + g^4[4T_{21}^{ci} + T_{22}^{ci}] + O(g^6), \quad (7.19)$$

where T_{11}^{ci} are given in Eq. (3.15) and (3.16) for $i = 1, 2$, respectively, while the two loop contributions are

$$T_{21}^{\text{c1}} = T_{21}^{\text{c1-c1}}, \quad T_{21}^{\text{c2}} = T_{21}^{\text{c2-c2}}, \quad T_{22}^{\text{c1}} = T_{22}^{\text{c1-c1}} + T_{22}^{\text{c1'-c1}}, \quad T_{22}^{\text{c2}} = T_{22}^{\text{c2-c2}} + T_{22}^{\text{c2-c2'}} \quad (7.20)$$

with the right-hand sides given in Eqs. (7.6) and (7.12). The region contribution $T_{22}^{\text{c2-c1}}$ is not included since it is given by the product of the one-loop T_{11}^{ci} 's,

$$T_{22}^{\text{c2-c1}} = 4T_{11}^{\text{c1}}T_{11}^{\text{c2}} + O(\varepsilon), \quad (7.21)$$

that emerges from the product J_1J_2 of one-loop contributions. Finally, the two-loop hard matching coefficient is

$$H = 1 + g^2[-2T_{11}^{\text{h}}] + g^4[4T_{21}^{\text{h-h}} + T_{22}^{\text{h-h}}] + O(g^6). \quad (7.22)$$

This coincides with the massless result by van Neerven [22]. All other mixed-region contributions should arise naturally in the product of factorized functions. However, this expectation turns out to be incorrect. There is a subtle mismatch between the two-loop ultra-soft–collinear regions and the product of one-loop ultrasoft and jet functions. Namely, the difference between Eqs. (2.2) and (6.1) is

$$\mathcal{F}_2 - \mathcal{F}_2^{\text{naive}} = (Z^2(\varepsilon) - 1) g^4 [-2T_{11}^{\text{us}}] [-2T_{11}^{\text{c1}} - T_{11}^{\text{c2}}], \quad (7.23)$$

where

$$Z^2(\varepsilon) = \frac{\Gamma(1 + 2\varepsilon)}{\Gamma^2(1 + \varepsilon)} = 1 + \zeta_2 \varepsilon^2 + O(\varepsilon^3). \quad (7.24)$$

Does this mean that our factorization formula (6.1) is doomed? Not quite.

7.2 Twisted functions and finite renormalization

Notice that $Z(\varepsilon)$ is accompanied by the one-loop components of the factorization formula, so we can *twist* them in such a manner that the desired factor of Z^2 arises in front of the product of ultrasoft and collinear functions, i.e.,

$$T_{11}^{\text{ci}} \rightarrow Z(\varepsilon) T_{11}^{\text{ci}}, \quad T_{11}^{\text{us}} \rightarrow Z(\varepsilon) T_{11}^{\text{us}}, \quad (7.25)$$

but it cannot affect the product of these with the hard function, so we have also to twist T_{11}^{h}

$$T_{11}^{\text{h}} \rightarrow Z^{-1}(\varepsilon) T_{11}^{\text{h}}. \quad (7.26)$$

But in these products, we have changed the finite parts of the one-loop functions involved (and their higher-order terms in the ε -expansion which is not relevant however at this loop order), so we have to perform a transformation to neutralize this twist. The only parameter we have at our disposal is the 't Hooft coupling. The required finite scheme transformation that does the trick is

$$g^2 \rightarrow g^2 (1 + 2\zeta_2 g^2 \mu^{2\varepsilon}). \quad (7.27)$$

This reminds of a ‘physical’ coupling that identifies the light-like cusp anomalous dimension as the new effective parameter of perturbative expansion⁸ [52, 53]. The twisted hard-matching coefficient and ultrasoft function are then

$$\mathcal{H} = (1 - 2\zeta_2 g^2 \mu^{2\varepsilon}) [1 + g^2 (1 + 2\zeta_2 g^2 \mu^{2\varepsilon}) [-2Z^{-1} T_{11}^{\text{h}}] + g^4 [4T_{21}^{\text{h-h}} + T_{22}^{\text{h-h}}] + O(g^6)], \quad (7.28)$$

$$\mathcal{S} = 1 + g^2 (1 + 2\zeta_2 g^2 \mu^{2\varepsilon}) [-2Z T_{11}^{\text{us}}] + g^4 [4T_{21}^{\text{us}} + T_{22}^{\text{us}}] + O(g^6), \quad (7.29)$$

where in the former we also corrected for the change in the absolute normalization. The same holds for the jet functions. For their product, we introduce

$$\mathcal{J}_1 \mathcal{J}_2 = 1 + g^2 (1 + 2\zeta_2 g^2 \mu^{2\varepsilon}) [-2Z T_{11}^{\text{c1}} - 2Z T_{11}^{\text{c2}}] \quad (7.30)$$

⁸We are grateful to Lorenzo Magnea for discussion of this point.

$$+ g^4[4T_{21}^{c1} + T_{22}^{c1} + 4T_{21}^{c2} + T_{22}^{c2} + T_{22}^{c2-c1}] + O(g^6).$$

Refactorization of their product into individual collinear components uses Eq. (7.21) and reads

$$\mathcal{J}_1 = 1 + g^2(1 + 2\zeta_2 g^2 \mu^{2\varepsilon})[-2ZT_{11}^{c1}] + g^4[4T_{21}^{c1} + T_{22}^{c1} + 2(1 - Z)[T_{11}^{c1}]^2] + O(g^6), \quad (7.31)$$

and the same for \mathcal{J}_2 with the obvious replacement $c1 \rightarrow c2$.

The final factorization formula for the off-shell Sudakov form factor then takes the same formal form as (6.1), where, however, one has to use the twisted form of individual functions with finite renormalization of the t Hooft coupling,

$$\mathcal{F}_2 = \mathcal{H}(\mu^2, \varepsilon) \mathcal{J}_1(\mu^2/m^2, \varepsilon) \mathcal{J}_2(\mu^2/m^2, \varepsilon) \mathcal{S}(\mu^2/m^4, \varepsilon). \quad (7.32)$$

Here, we do not display the ultrasoft jets since they are all unity in dimensional regularization employed in our formalism.

8 Evolution equations

Let us close this paper with a discussion of the renormalization and infrared evolution equations.

8.1 Renormalization group

While the total Sudakov form factor \mathcal{F}_2 is a finite quantity, its incoherent momentum components possess divergences in the parameter of dimensional regularization ε . They are infrared for \mathcal{H} , ultraviolet for \mathcal{S} , and mixed for the jet functions \mathcal{J}_i canceling in their product. We can use the independence of \mathcal{F}_2 on the renormalization scale μ to derive renormalization group equations for them.

Let us define the renormalized functions in the minimal subtraction scheme as

$$\mathcal{H} = \mathcal{Z}_h \mathcal{H}_R, \quad \mathcal{J}_i = \mathcal{Z}_{\text{col}} \mathcal{J}_{i,R}, \quad \mathcal{S} = \mathcal{Z}_{\text{us}} \mathcal{S}_R, \quad (8.1)$$

where to the two-loop order

$$\log \mathcal{Z}_h = g^2 \left[-\frac{2}{\varepsilon^2} - \frac{2}{\varepsilon} \log \mu^2 \right] + g^4 \left[-\frac{\zeta_2}{\varepsilon^2} - \frac{2\zeta_2}{\varepsilon} \log \mu^2 - \frac{3\zeta_3}{\varepsilon} \right], \quad (8.2)$$

$$\log \mathcal{Z}_{\text{col}} = g^2 \left[\frac{2}{\varepsilon^2} + \frac{2}{\varepsilon} \log \mu^2 - \frac{2}{\varepsilon} \log m^2 \right] + g^4 \left[\frac{\zeta_2}{\varepsilon^2} + \frac{2\zeta_2}{\varepsilon} \log \mu^2 + \frac{2\zeta_2}{\varepsilon} \log m^2 + \frac{3\zeta_3}{\varepsilon} \right], \quad (8.3)$$

$$\log \mathcal{Z}_{\text{us}} = g^2 \left[-\frac{2}{\varepsilon^2} - \frac{2}{\varepsilon} \log \mu^2 + \frac{4}{\varepsilon} \log m^2 \right] + g^4 \left[-\frac{\zeta_2}{\varepsilon^2} - \frac{2\zeta_2}{\varepsilon} \log \mu^2 - \frac{4\zeta_2}{\varepsilon} \log m^2 - \frac{3\zeta_3}{\varepsilon} \right]. \quad (8.4)$$

After these subtractions, the logarithms of the renormalized functions admit the form

$$\log \mathcal{H}_R(\mu^2) = -g^2 \log^2 \mu^2 + g^4 \left[-2\zeta_2 \log^2 \mu^2 - 6\zeta_3 \log \mu^2 + \frac{9\zeta_4}{2} \right], \quad (8.5)$$

$$\begin{aligned} \log \mathcal{J}_{i,R}(\mu^2, m^2) &= g^2 [\log^2 \mu^2 - 2 \log \mu^2 \log m^2 + \log^2 m^2] \\ &+ g^4 \left[2\zeta_2 \log^2 \mu^2 + 4\zeta_2 \log \mu^2 \log m^2 - 4\zeta_2 \log^2 m^2 \right. \\ &\quad \left. + 6\zeta_3 \log \mu^2 - 6\zeta_3 \log m^2 + \frac{\zeta_4}{2} \right], \end{aligned} \quad (8.6)$$

$$\begin{aligned} \log \mathcal{S}_R(\mu^2, m^2) &= g^2 [-\log^2 \mu^2 + 4 \log \mu^2 \log m^2 - 4 \log^2 m^2 - 4\zeta_2] \\ &+ g^4 \left[-2\zeta_2 \log^2 \mu^2 - 8\zeta_2 \log \mu^2 \log m^2 + 16\zeta_2 \log^2 m^2 \right. \\ &\quad \left. - 6\zeta_3 \log \mu^2 + 12\zeta_3 \log m^2 + \frac{53\zeta_4}{2} \right]. \end{aligned} \quad (8.7)$$

Defining the anomalous dimensions with a conventional equation,

$$\gamma = -\frac{d \log \mathcal{Z}}{d \log \mu^2}, \quad (8.8)$$

we immediately deduce their two-loop form

$$\gamma_h = g^2 [-2 \log \mu^2] + g^4 [-4\zeta_2 \log \mu^2 - 6\zeta_3], \quad (8.9)$$

$$\gamma_{\text{col}} = g^2 [2 \log \mu^2 - 2 \log m^2] + g^4 [4\zeta_2 \log \mu^2 + 4\zeta_2 \log m^2 + 6\zeta_3], \quad (8.10)$$

$$\gamma_{\text{us}} = g^2 [-2 \log \mu^2 + 4 \log m^2] + g^4 [-4\zeta_2 \log \mu^2 - 8\zeta_2 \log m^2 - 6\zeta_3]. \quad (8.11)$$

Here we used the fact that the 't Hooft coupling (2.6) is running in D -dimensions $dg/d \log \mu^2 = -\varepsilon g/2$. These anomalous dimensions are not independent and obey the equation

$$\gamma_h + 2\gamma_{\text{col}} + \gamma_{\text{us}} = 0 \quad (8.12)$$

as a consequence of μ -independence of \mathcal{F}_2 . Notice that due to the fact that the ultrasoft function is not scaleless, there is a mismatch between the infrared and ultraviolet logarithms. So contrary to the massless case, where the study of ultraviolet renormalization properties of vacuum expectation values of Wilson lines can be used to study infrared physics, this is no longer the case for the off-shell case.

8.2 Infrared evolution

Now we are in a position to derive evolution equations in the infrared scale m . In this section, we set $\mu = 1$, i.e., μ set equal to the hard scale Q in terms of the original dimensionful μ . Making use of Eqs. (8.6) and (8.7), the dependence on m is driven by the relations

$$\frac{d \log \mathcal{J}_{i,R}(1, m^2)}{d \log m^2} = \frac{1}{2} \Gamma_{\text{oct}}(g) \log m^2 + \Gamma_{\text{col}}(g), \quad (8.13)$$

$$\frac{d \log \mathcal{S}_R(1, m^2)}{d \log m^2} = -2\Gamma_{\text{oct}}(g) \log m^2 - 2\Gamma_{\text{col}}(g), \quad (8.14)$$

with the octagon anomalous dimension accompanying the logarithm (2.9) and the collinear anomalous dimension for the log-free term,

$$\Gamma_{\text{col}}(g) = -6\zeta_3 g^4 + O(g^6). \quad (8.15)$$

It is not the on-shell collinear anomalous dimension, $\Gamma_{\text{col}}^{\text{on-shell}}(g) = -4\zeta_3 g^4 + O(g^6)$! The contribution from Γ_{col} cancels however in the evolution equation for the Sudakov form factor \mathcal{F}_2 such it does not possess a single logarithmic term to any order of perturbation theory.

8.3 Untwisted vs. twisted

Finally, let us comment on the evolution equation for the untwisted ultrasoft functions S . It was proposed in Ref. [5] that its dependence on the ultrasoft scale μ_{us} (6.3) is governed by the ubiquitous cusp anomalous dimension. We can now verify this statement using our explicit two-loop result. We find from Eq. (5.33) for its renormalized counterpart ($\mu = 1$)

$$\log S_{\text{R}}(\mu_{\text{us}}) = g^2 [-4 \log^2 \mu_{\text{us}} - 3\zeta_2] + g^4 [40\zeta_2 \log^2 \mu_{\text{us}} + 28\zeta_3 \log \mu_{\text{us}} + 71\zeta_4] + O(g^6), \quad (8.16)$$

and thus

$$\frac{\log S_{\text{R}}(\mu_{\text{us}})}{d \log \mu_{\text{us}}} = -2 [4g^2 - 40\zeta_2] \log \mu_{\text{us}} - 28\zeta_3 g^4 + O(g^6). \quad (8.17)$$

We observe that the function of the gauge coupling in front of $\log \mu_{\text{us}}$ is not proportional to Γ_{cusp} . Let us point out, however, that if we modify the structure of the evolution equation by allowing a convolution term in its right-hand side, we can then recover the perturbative expansion of Eq. (8.16) with just the cusp anomalous dimension alone (and a new collinear one). Namely,

$$\frac{dS_{\text{R}}(\mu_{\text{us}})}{d \log \mu_{\text{us}}} = -[2\Gamma_{\text{cusp}}(g) \log \mu_{\text{us}} + \tilde{\Gamma}(g)]S_{\text{R}}(\mu_{\text{us}}) - 2\Gamma_{\text{cusp}}(g) \int_0^{\mu_{\text{us}}} d\mu'_{\text{us}} \frac{S_{\text{R}}(\mu'_{\text{us}}) - S_{\text{R}}(\mu_{\text{us}})}{\mu'_{\text{us}} - \mu_{\text{us}}}, \quad (8.18)$$

with $\Gamma_{\text{cusp}}(g) = 4g^2 - 8\zeta_2 g^4 + O(g^6)$ and $\tilde{\Gamma}(g) = -92\zeta_3 g^4 + O(g^6)$. The same can be done with Eqs. (8.13), (8.14) but only making use of two different anomalous dimensions $\tilde{\Gamma}(g)$, which is quite unnatural considering the fact that the log-free portion of the evolution equation should be absent for the total form factor.

9 Conclusions

In this paper, we continued our exploration of the Sudakov form factor on the Coulomb branch of $\mathcal{N} = 4$ sYM. We analyzed its factorization in terms of incoherent components responsible for physics at different momentum scales, from hard to ultrasoft. The main mathematical tool at our disposal was MofR which allowed us to identify various contributions to Feynman integrals in terms of essential momentum modes. However, when we attempted to naively separate these in terms of the jet and ultrasoft functions, and a hard matching coefficient, we encountered a predicament at subleading orders in the ε -expansion: there was a ‘non-factorizable’ leftover. We, however, managed to twist the functions involved

along with a finite renormalization of the 't Hooft coupling to rescue our factorization formula. The question remains whether this can be done to all orders. It is nevertheless puzzling that while the complete form factor admits a very simple form in the near mass-shell limit, its factorization does not enjoy the simplicity of its on-shell counterpart, which is a far more complex function of the 't Hooft coupling, though not so different in kinematical dependence. Are we missing an integral convolution in disguise between different factorized components that would accommodate the deviation we observed in our two-loop analysis? This would, of course, be quite a departure from the familiar on-shell story. This question begs for further studies. Currently, this question is under study at three-loop order.

Acknowledgments

We are grateful to Lorenzo Magnea for reading the manuscript and providing instructive comments. The work of A.B. was supported by the U.S. National Science Foundation under grant No. PHY-2207138. The work of L.B. was supported by the Foundation for the Advancement of Theoretical Physics and Mathematics “BASIS”. The work of V.S. was supported by the Russian Science Foundation under the agreement No. 21-71-30003.

A Light-cone singularity of scalar propagator

As in the main body of the paper, we adopt notations from Ref. [54] for $\mathcal{N} = 4$ sYM Lagrangian and fields populating it. We consider the exact scalar propagator in the external long-wavelength gauge field A and expand it to the linear order in g

$$S_{ab}^{ABCD}(x_2, x_1) = \langle \phi_a^{AB}(x_2) \phi_b^{CD}(x_1) \rangle_A = \delta_{ab} S_{(0)}^{ABCD}(x_2, x_1) + S_{(1)ab}^{ABCD}(x_2, x_1) + \dots, \quad (\text{A.1})$$

where the leading term is the bare propagator

$$S_{(0)}^{ABCD}(x_2, x_1) = -\varepsilon_{ABCD} \frac{1}{4\pi^{D/2}} \frac{\Gamma(D/2 - 1)}{[-x_{12}^2]^{D/2-1}}, \quad (\text{A.2})$$

while the first correction takes the form of the vacuum expectation value with the gauge-scalar-scalar vertex V_s

$$\begin{aligned} S_{(1)ab}^{ABCD}(x_2, x_1) &= \langle \phi_a^{AB}(x_2) \phi_b^{CD}(x_1) i \int d^D x_0 V_s(x_0) \rangle \\ &= \frac{ig}{16\pi^D} f_{abc} \varepsilon^{ABCD} (\partial_2 - \partial_1)_\mu \int d^D x_0 A_\mu^a(x_0) \frac{\Gamma(D/2 - 1)}{[-x_{10}^2]^{D/2-1}} \frac{\Gamma(D/2 - 1)}{[-x_{20}^2]^{D/2-1}}. \end{aligned} \quad (\text{A.3})$$

The integral can be easily calculated

$$\int d^D x_0 A_\mu^a(x_0) \frac{\Gamma(D/2 - 1)}{[-x_{10}^2]^{D/2-1}} \frac{\Gamma(D/2 - 1)}{[-x_{20}^2]^{D/2-1}}$$

$$\begin{aligned}
&= \int_0^1 d\sigma (\sigma \bar{\sigma})^{D/2-2} \int d^D x_0 A_\mu^a(x_0 + \sigma x_2 + \bar{\sigma} x_1) \frac{\Gamma(D-1)}{[-x_0^2 - \sigma \bar{\sigma} x_{12}^2]^{D-2}} \\
&= -i\pi^{D/2} \frac{\Gamma(D/2-1)}{[-x_{12}^2]^{D/2-2}} \int_0^1 d\sigma A_\mu^a(\sigma x_2 + \bar{\sigma} x_1), \tag{A.4}
\end{aligned}$$

where $\bar{\sigma} \equiv 1 - \sigma$ and in the second step we performed the expansion of $A_\mu(x_0 + \sigma x_2 + \bar{\sigma} x_1)$ in the Taylor series around $x_0 = 0$ using the long wavelength approximation and eliminated higher-twist effects. In this manner, we find for the leading light-cone singularity of $O(A)$ correction to the scalar propagator

$$S_{(1)ab}^{ABCD}(x_2, x_1) = S_{(0)}^{ABCD}(x_2, x_1) \left(ig \int_0^1 d\sigma x_{12}^\mu (A_\mu)^{ab}(\sigma x_2 + \bar{\sigma} x_1) \right), \tag{A.5}$$

with the adjoint matrix of gauge fields $(A_\mu)^{ab} = A_\mu^c (T^c)_{ab}$. Performing identical manipulations for terms of $O(A^2)$ and higher, we uncover the known expression for the light-cone singularity of the propagator in the external field [55]

$$S_{(1)ab}^{ABCD}(x_2, x_1) = S_{(0)}^{ABCD}(x_2, x_1)[x_2, x_1], \tag{A.6}$$

with the Wilson line segment defined in Eq. (5.2).

B Region integrals at two loops

In this appendix, we present contributions from separate regions to the two-loop ladder and cross-ladder integrals. Their Feynman-parameter representations read for T_{21}

$$\begin{aligned}
T_{21}^{\text{h-h}} &= e^{2\varepsilon\gamma_E} \mu^{4\varepsilon} \Gamma(2+2\varepsilon) \\
&\times \int d^6 \mathbf{x} (x_1 x_2 + x_2 x_3 + x_1 x_4 + x_2 x_4 + x_3 x_4 + x_2 x_5 + x_4 x_5 + x_1 x_6 + x_2 x_6 + x_3 x_6 + x_5 x_6)^{3\varepsilon} \\
&\times (x_2 x_3 x_5 + x_2 x_4 x_5 + x_3 x_4 x_5 + x_2 x_3 x_6 + x_1 x_4 x_6 + x_2 x_4 x_6 + x_3 x_4 x_6 + x_3 x_5 x_6 + x_4 x_5 x_6)^{-2-2\varepsilon}, \tag{B.1}
\end{aligned}$$

$$\begin{aligned}
T_{21}^{\text{h-c1}} &= e^{2\varepsilon\gamma_E} \left(\frac{\mu^4}{m^2} \right)^\varepsilon \Gamma(2+2\varepsilon) \\
&\times \int d^6 \mathbf{x} (x_1 x_2 + x_2 x_3 + x_1 x_4 + x_3 x_4 + x_1 x_6 + x_3 x_6)^{3\varepsilon} \\
&\times (x_1 x_2 x_3 + x_1 x_3 x_4 + x_2 x_3 x_5 + x_3 x_4 x_5 + x_1 x_3 x_6 + x_2 x_3 x_6 + x_1 x_4 x_6 + x_3 x_4 x_6 + x_3 x_5 x_6)^{-2-2\varepsilon}, \tag{B.2}
\end{aligned}$$

$$\begin{aligned}
T_{21}^{\text{h-c2}} &= e^{2\varepsilon\gamma_E} \left(\frac{\mu^4}{m^2} \right)^\varepsilon \Gamma(2+2\varepsilon) \\
&\times \int d^6 \mathbf{x} (x_1 x_2 + x_1 x_4 + x_2 x_5 + x_4 x_5 + x_1 x_6 + x_5 x_6)^{3\varepsilon} \\
&\times (x_1 x_2 x_5 + x_2 x_3 x_5 + x_1 x_4 x_5 + x_2 x_4 x_5 + x_3 x_4 x_5 + x_1 x_4 x_6 + x_1 x_5 x_6 + x_3 x_5 x_6 + x_4 x_5 x_6)^{-2-2\varepsilon}, \tag{B.3}
\end{aligned}$$

$$\begin{aligned}
T_{21}^{\text{c1-c1}} &= e^{2\varepsilon\gamma_E} \left(\frac{\mu^2}{m^2} \right)^{2\varepsilon} \Gamma(2+2\varepsilon) \\
&\times \int d^6 \mathbf{x} (x_1 x_2 + x_2 x_3 + x_1 x_4 + x_2 x_4 + x_3 x_4)^{3\varepsilon} \tag{B.4}
\end{aligned}$$

$$\begin{aligned}
& \times (x_1x_2x_3 + x_1x_2x_4 + x_1x_3x_4 + x_2x_3x_5 + x_2x_4x_5 + x_3x_4x_5 + x_2x_3x_6 + x_1x_4x_6 + x_2x_4x_6 + x_3x_4x_6)^{-2-2\varepsilon}, \\
T_{21}^{\text{c2-c2}} &= e^{2\varepsilon\gamma_E} \left(\frac{\mu^2}{m^2}\right)^{2\varepsilon} \Gamma(2+2\varepsilon) \tag{B.5}
\end{aligned}$$

$$\begin{aligned}
& \times \int d^6\mathbf{x} (x_1x_2 + x_2x_5 + x_1x_6 + x_2x_6 + x_5x_6)^{3\varepsilon} \\
& \times (x_1x_2x_5 + x_2x_3x_5 + x_2x_4x_5 + x_1x_2x_6 + x_2x_3x_6 + x_1x_4x_6 + x_2x_4x_6 + x_1x_5x_6 + x_3x_5x_6 + x_4x_5x_6)^{-2-2\varepsilon}, \\
T_{21}^{\text{h-us}} &= e^{2\varepsilon\gamma_E} \left(\frac{\mu^4}{m^4}\right)^\varepsilon \Gamma(2+2\varepsilon) \tag{B.6}
\end{aligned}$$

$$\begin{aligned}
& \times \int d^6\mathbf{x} (x_1x_2 + x_1x_4 + x_1x_6)^{3\varepsilon} \\
& \times (x_1x_2x_3 + x_1x_3x_4 + x_1x_2x_5 + x_2x_3x_5 + x_1x_4x_5 + x_3x_4x_5 + x_1x_3x_6 + x_1x_4x_6 + x_1x_5x_6 + x_3x_5x_6)^{-2-2\varepsilon}, \\
T_{21}^{\text{c1-us}} &= e^{2\varepsilon\gamma_E} \left(\frac{\mu^4}{m^6}\right)^\varepsilon \Gamma(2+2\varepsilon) \tag{B.7}
\end{aligned}$$

$$\begin{aligned}
& \times \int d^6\mathbf{x} (x_1x_2 + x_1x_4)^{3\varepsilon} \\
& \times (x_1x_2x_3 + x_1x_2x_4 + x_1x_3x_4 + x_1x_2x_5 + x_2x_3x_5 + x_1x_4x_5 + x_2x_4x_5 + x_3x_4x_5 + x_1x_4x_6)^{-2-2\varepsilon}, \\
T_{21}^{\text{c2-us}} &= e^{2\varepsilon\gamma_E} \left(\frac{\mu^4}{m^6}\right)^\varepsilon \Gamma(2+2\varepsilon) \tag{B.8}
\end{aligned}$$

$$\begin{aligned}
& \times \int d^6\mathbf{x} (x_1x_2 + x_1x_6)^{3\varepsilon} \\
& \times (x_1x_2x_3 + x_1x_2x_5 + x_2x_3x_5 + x_1x_2x_6 + x_1x_3x_6 + x_2x_3x_6 + x_1x_4x_6 + x_1x_5x_6 + x_3x_5x_6)^{-2-2\varepsilon}, \\
T_{21}^{\text{us-us}} &= e^{2\varepsilon\gamma_E} \left(\frac{\mu^2}{m^4}\right)^{2\varepsilon} \Gamma(2+2\varepsilon) \tag{B.9} \\
& \times \int d^6\mathbf{x} (x_1x_2)^{3\varepsilon} \\
& \times (x_1x_2x_3 + x_1x_2x_4 + x_1x_2x_5 + x_2x_3x_5 + x_2x_4x_5 + x_1x_2x_6 + x_2x_3x_6 + x_1x_4x_6 + x_2x_4x_6)^{-2-2\varepsilon},
\end{aligned}$$

and T_{22}

$$\begin{aligned}
T_{22}^{\text{h-h}} &= e^{2\varepsilon\gamma_E} \mu^{4\varepsilon} \Gamma(2+2\varepsilon) \tag{B.10} \\
& \times \int d^6\mathbf{x} (x_1x_2 + x_2x_3 + x_1x_4 + x_2x_4 + x_3x_4 + x_1x_5 + x_2x_5 + x_3x_5 + x_1x_6 + x_3x_6 + x_4x_6 + x_5x_6)^{3\varepsilon} \\
& \times (x_2x_3x_5 + x_1x_4x_5 + x_2x_4x_5 + x_3x_4x_5 + x_1x_4x_6 + x_4x_5x_6)^{-2-2\varepsilon},
\end{aligned}$$

$$\begin{aligned}
T_{22}^{\text{c2-h}} &= e^{2\varepsilon\gamma_E} \left(\frac{\mu^4}{m^2}\right)^\varepsilon \Gamma(2+2\varepsilon) \tag{B.11} \\
& \times \int d^6\mathbf{x} (x_1x_2 + x_2x_3 + x_2x_4 + x_2x_5 + x_1x_6 + x_3x_6 + x_4x_6 + x_5x_6)^{3\varepsilon} \\
& \times (x_2x_3x_5 + x_2x_4x_5 + x_1x_2x_6 + x_2x_3x_6 + x_1x_4x_6 + x_2x_4x_6 + x_2x_5x_6 + x_4x_5x_6)^{-2-2\varepsilon},
\end{aligned}$$

$$\begin{aligned}
T_{22}^{\text{h-c1}} &= e^{2\varepsilon\gamma_E} \left(\frac{\mu^4}{m^2}\right)^\varepsilon \Gamma(2+2\varepsilon) \tag{B.12} \\
& \times \int d^6\mathbf{x} (x_1x_2 + x_2x_3 + x_1x_4 + x_3x_4 + x_1x_5 + x_3x_5 + x_1x_6 + x_3x_6)^{3\varepsilon} \\
& \times (x_1x_2x_3 + x_1x_3x_4 + x_1x_3x_5 + x_2x_3x_5 + x_1x_4x_5 + x_3x_4x_5 + x_1x_3x_6 + x_1x_4x_6)^{-2-2\varepsilon},
\end{aligned}$$

$$T_{22}^{\text{c2-c2}} = e^{2\varepsilon\gamma_E} \left(\frac{\mu^2}{m^2}\right)^{2\varepsilon} \Gamma(2+2\varepsilon) \tag{B.13}$$

$$\begin{aligned}
& \times \int d^6 \mathbf{x} (x_1 x_2 + x_1 x_5 + x_2 x_5 + x_1 x_6 + x_5 x_6)^{3\varepsilon} \\
& \times (x_1 x_2 x_5 + x_2 x_3 x_5 + x_1 x_4 x_5 + x_2 x_4 x_5 + x_1 x_2 x_6 + x_1 x_4 x_6 + x_2 x_5 x_6 + x_4 x_5 x_6)^{-2-2\varepsilon}, \\
T_{22}^{\text{cl}'-\text{cl}} &= e^{2\varepsilon\gamma_E} \left(\frac{\mu^2}{m^2}\right)^{2\varepsilon} \Gamma(2+2\varepsilon) \tag{B.14}
\end{aligned}$$

$$\begin{aligned}
& \times \int d^6 \mathbf{x} (x_1 x_5 + x_3 x_5 + x_1 x_6 + x_3 x_6 + x_5 x_6)^{3\varepsilon} \\
& \times (x_1 x_3 x_5 + x_2 x_3 x_5 + x_1 x_4 x_5 + x_3 x_4 x_5 + x_1 x_3 x_6 + x_1 x_4 x_6 + x_3 x_5 x_6 + x_4 x_5 x_6)^{-2-2\varepsilon}, \\
T_{22}^{\text{c2}-\text{cl}} &= e^{2\varepsilon\gamma_E} \left(\frac{\mu^2}{m^2}\right)^{2\varepsilon} \Gamma(2+2\varepsilon) \tag{B.15}
\end{aligned}$$

$$\begin{aligned}
& \times \int d^6 \mathbf{x} (x_1 x_2 + x_2 x_3 + x_1 x_6 + x_3 x_6)^{3\varepsilon} \\
& \times (x_1 x_2 x_3 + x_2 x_3 x_5 + x_1 x_2 x_6 + x_1 x_3 x_6 + x_2 x_3 x_6 + x_1 x_4 x_6)^{-2-2\varepsilon}, \\
T_{22}^{\text{cl}-\text{cl}} &= e^{2\varepsilon\gamma_E} \left(\frac{\mu^2}{m^2}\right)^{2\varepsilon} \Gamma(2+2\varepsilon) \tag{B.16}
\end{aligned}$$

$$\begin{aligned}
& \times \int d^6 \mathbf{x} (x_1 x_2 + x_2 x_3 + x_1 x_4 + x_2 x_4 + x_3 x_4)^{3\varepsilon} \\
& \times (x_1 x_2 x_3 + x_1 x_2 x_4 + x_1 x_3 x_4 + x_2 x_3 x_5 + x_1 x_4 x_5 + x_2 x_4 x_5 + x_3 x_4 x_5 + x_1 x_4 x_6)^{-2-2\varepsilon}, \\
T_{22}^{\text{c2}-\text{c2}'} &= e^{2\varepsilon\gamma_E} \left(\frac{\mu^2}{m^2}\right)^{2\varepsilon} \Gamma(2+2\varepsilon) \tag{B.17}
\end{aligned}$$

$$\begin{aligned}
& \times \int d^6 \mathbf{x} (x_2 x_3 + x_2 x_4 + x_3 x_4 + x_3 x_6 + x_4 x_6)^{3\varepsilon} \\
& \times (x_2 x_3 x_5 + x_2 x_4 x_5 + x_3 x_4 x_5 + x_2 x_3 x_6 + x_1 x_4 x_6 + x_2 x_4 x_6 + x_3 x_4 x_6 + x_4 x_5 x_6)^{-2-2\varepsilon}, \\
T_{22}^{\text{us}'-\text{cl}} &= e^{2\varepsilon\gamma_E} \left(\frac{\mu^4}{m^6}\right)^\varepsilon \Gamma(2+2\varepsilon) \tag{B.18}
\end{aligned}$$

$$\begin{aligned}
& \times \int d^6 \mathbf{x} (x_1 x_6 + x_3 x_6 + x_5 x_6)^{3\varepsilon} \\
& \times (x_2 x_3 x_5 + x_1 x_2 x_6 + x_1 x_3 x_6 + x_2 x_3 x_6 + x_1 x_4 x_6 + x_2 x_5 x_6 + x_3 x_5 x_6 + x_4 x_5 x_6)^{-2-2\varepsilon}, \\
T_{22}^{\text{c2}-\text{us}} &= e^{2\varepsilon\gamma_E} \left(\frac{\mu^4}{m^6}\right)^\varepsilon \Gamma(2+2\varepsilon) \tag{B.19}
\end{aligned}$$

$$\begin{aligned}
& \times \int d^6 \mathbf{x} (x_1 x_2 + x_1 x_5 + x_1 x_6)^{3\varepsilon} \\
& \times (x_1 x_2 x_3 + x_1 x_2 x_5 + x_1 x_3 x_5 + x_2 x_3 x_5 + x_1 x_4 x_5 + x_1 x_2 x_6 + x_1 x_3 x_6 + x_1 x_4 x_6)^{-2-2\varepsilon}, \\
T_{22}^{\text{us}-\text{cl}} &= e^{2\varepsilon\gamma_E} \left(\frac{\mu^4}{m^6}\right)^\varepsilon \Gamma(2+2\varepsilon) \tag{B.20}
\end{aligned}$$

$$\begin{aligned}
& \times \int d^6 \mathbf{x} (x_1 x_2 + x_2 x_3 + x_2 x_4)^{3\varepsilon} \\
& \times (x_1 x_2 x_3 + x_1 x_2 x_4 + x_2 x_3 x_5 + x_2 x_4 x_5 + x_1 x_2 x_6 + x_2 x_3 x_6 + x_1 x_4 x_6 + x_2 x_4 x_6)^{-2-2\varepsilon}, \\
T_{22}^{\text{c2}-\text{us}'} &= e^{2\varepsilon\gamma_E} \left(\frac{\mu^4}{m^6}\right)^\varepsilon \Gamma(2+2\varepsilon) \tag{B.21}
\end{aligned}$$

$$\begin{aligned}
& \times \int d^6 \mathbf{x} (x_2 x_3 + x_3 x_4 + x_3 x_6)^{3\varepsilon} \\
& \times (x_1 x_2 x_3 + x_1 x_3 x_4 + x_2 x_3 x_5 + x_3 x_4 x_5 + x_1 x_3 x_6 + x_2 x_3 x_6 + x_1 x_4 x_6 + x_3 x_4 x_6)^{-2-2\varepsilon}, \\
T_{22}^{\text{us}'-\text{us}'} &= e^{2\varepsilon\gamma_E} \left(\frac{\mu^2}{m^4}\right)^{2\varepsilon} \Gamma(2+2\varepsilon) \tag{B.22}
\end{aligned}$$

$$\begin{aligned}
& \times \int d^6 \mathbf{x} (x_3 x_6)^{3\epsilon} \\
& \times (x_2 x_3 x_5 + x_3 x_4 x_5 + x_1 x_3 x_6 + x_2 x_3 x_6 + x_1 x_4 x_6 + x_3 x_4 x_6 + x_3 x_5 x_6 + x_4 x_5 x_6)^{-2-2\epsilon}, \\
T_{22}^{\text{us-us}} &= e^{2\epsilon\gamma_E} \left(\frac{\mu^2}{m^4}\right)^{2\epsilon} \Gamma(2+2\epsilon) \tag{B.23} \\
& \times \int d^6 \mathbf{x} (x_1 x_2)^{3\epsilon} \\
& \times (x_1 x_2 x_3 + x_1 x_2 x_4 + x_1 x_2 x_5 + x_2 x_3 x_5 + x_1 x_4 x_5 + x_2 x_4 x_5 + x_1 x_2 x_6 + x_1 x_4 x_6)^{-2-2\epsilon},
\end{aligned}$$

$$\begin{aligned}
T_{22}^{\text{us}'\text{-us}} &= e^{2\epsilon\gamma_E} \left(\frac{\mu^2}{m^4}\right)^{2\epsilon} \Gamma(2+2\epsilon) \tag{B.24} \\
& \times \int d^6 \mathbf{x} (x_1 x_5 + x_1 x_6 + x_5 x_6)^{3\epsilon} \\
& \times (x_1 x_2 x_5 + x_1 x_3 x_5 + x_2 x_3 x_5 + x_1 x_4 x_5 + x_1 x_2 x_6 + x_1 x_3 x_6 + x_1 x_4 x_6 + x_2 x_5 x_6 + x_3 x_5 x_6 + x_4 x_5 x_6)^{-2-2\epsilon},
\end{aligned}$$

$$\begin{aligned}
T_{22}^{\text{us-us}'} &= e^{2\epsilon\gamma_E} \left(\frac{\mu^2}{m^4}\right)^{2\epsilon} \Gamma(2+2\epsilon) \tag{B.25} \\
& \times \int d^6 \mathbf{x} (x_2 x_3 + x_2 x_4 + x_3 x_4)^{3\epsilon} \\
& \times (x_1 x_2 x_3 + x_1 x_2 x_4 + x_1 x_3 x_4 + x_2 x_3 x_5 + x_2 x_4 x_5 + x_3 x_4 x_5 + x_2 x_3 x_6 + x_1 x_4 x_6 + x_2 x_4 x_6 + x_3 x_4 x_6)^{-2-2\epsilon},
\end{aligned}$$

respectively.

References

- [1] A. V. Belitsky, L. V. Bork, A. F. Pikelner and V. A. Smirnov, *Exact Off Shell Sudakov Form Factor in $N=4$ Supersymmetric Yang-Mills Theory*, *Phys. Rev. Lett.* **130** (2023) 091605, [[2209.09263](#)].
- [2] A. V. Belitsky, L. V. Bork and V. A. Smirnov, *Off-shell form factor in $\mathcal{N}=4$ sYM at three loops*, *JHEP* **11** (2023) 111, [[2306.16859](#)].
- [3] A. V. Belitsky and G. P. Korchemsky, *Exact null octagon*, *JHEP* **05** (2020) 070, [[1907.13131](#)].
- [4] A. H. Mueller, *On the Asymptotic Behavior of the Sudakov Form-factor*, *Phys. Rev. D* **20** (1979) 2037.
- [5] G. P. Korchemsky, *Sudakov Form-factor in QCD*, *Phys. Lett. B* **220** (1989) 629–634.
- [6] S. Forte, *On the Sudakov form factor, and a factor of two*, 2020. [2001.04995](#).
- [7] L. D. Landau, *On analytic properties of vertex parts in quantum field theory*, *Nucl. Phys.* **13** (1959) 181–192.
- [8] S. Coleman and R. E. Norton, *Singularities in the physical region*, *Nuovo Cim.* **38** (1965) 438–442.
- [9] M. Beneke and V. A. Smirnov, *Asymptotic expansion of Feynman integrals near threshold*, *Nucl. Phys. B* **522** (1998) 321–344, [[hep-ph/9711391](#)].
- [10] V. A. Smirnov, *Expansion by Regions: An Overview*. 2021. [2406.11475](#).

- [11] A. V. Manohar and I. W. Stewart, *The Zero-Bin and Mode Factorization in Quantum Field Theory*, *Phys. Rev. D* **76** (2007) 074002, [[hep-ph/0605001](#)].
- [12] L. J. Dixon, L. Magnea and G. F. Sterman, *Universal structure of subleading infrared poles in gauge theory amplitudes*, *JHEP* **08** (2008) 022, [[0805.3515](#)].
- [13] N. Agarwal, L. Magnea, C. Signorile-Signorile and A. Tripathi, *The infrared structure of perturbative gauge theories*, *Phys. Rept.* **994** (2023) 1–120, [[2112.07099](#)].
- [14] J. C. Collins, *Sudakov form-factors*, *Adv. Ser. Direct. High Energy Phys.* **5** (1989) 573–614, [[hep-ph/0312336](#)].
- [15] G. P. Korchemsky and A. V. Radyushkin, *Renormalization of the Wilson Loops Beyond the Leading Order*, *Nucl. Phys. B* **283** (1987) 342–364.
- [16] E. Gardi and L. Magnea, *Factorization constraints for soft anomalous dimensions in QCD scattering amplitudes*, *JHEP* **03** (2009) 079, [[0901.1091](#)].
- [17] V. Del Duca, *High-energy Bremsstrahlung Theorems for Soft Photons*, *Nucl. Phys. B* **345** (1990) 369–388.
- [18] D. Bonocore, E. Laenen, L. Magnea, L. Vernazza and C. D. White, *The method of regions and next-to-soft corrections in Drell–Yan production*, *Phys. Lett. B* **742** (2015) 375–382, [[1410.6406](#)].
- [19] S. Caron-Huot and F. Coronado, *Ten dimensional symmetry of $\mathcal{N} = 4$ SYM correlators*, *JHEP* **03** (2022) 151, [[2106.03892](#)].
- [20] L. F. Alday, J. M. Henn, J. Plefka and T. Schuster, *Scattering into the fifth dimension of $N=4$ super Yang-Mills*, *JHEP* **01** (2010) 077, [[0908.0684](#)].
- [21] T. Gehrmann, J. M. Henn and T. Huber, *The three-loop form factor in $N=4$ super Yang-Mills*, *JHEP* **03** (2012) 101, [[1112.4524](#)].
- [22] W. L. van Neerven, *Infrared Behavior of On-shell Form-factors in a $N = 4$ Supersymmetric Yang-Mills Field Theory*, *Z. Phys. C* **30** (1986) 595.
- [23] L. V. Bork, D. I. Kazakov and G. S. Vartanov, *On form factors in $N=4$ SYM*, *JHEP* **02** (2011) 063, [[1011.2440](#)].
- [24] R. Jackiw, *Dynamics at high momentum and the vertex function of spinor electrodynamics*, *Annals Phys.* **48** (1968) 292–321.
- [25] V. V. Sudakov, *Vertex parts at very high-energies in quantum electrodynamics*, *Sov. Phys. JETP* **3** (1956) 65–71.
- [26] W. Siegel, *Supersymmetric Dimensional Regularization via Dimensional Reduction*, *Phys. Lett. B* **84** (1979) 193–196.
- [27] J. M. Henn, *Multiloop integrals in dimensional regularization made simple*, *Phys. Rev. Lett.* **110** (2013) 251601, [[1304.1806](#)].
- [28] B. Jantzen, *Foundation and generalization of the expansion by regions*, *JHEP* **12** (2011) 076, [[1111.2589](#)].

- [29] G. F. Sterman, *Mass Divergences in Annihilation Processes. 1. Origin and Nature of Divergences in Cut Vacuum Polarization Diagrams*, *Phys. Rev. D* **17** (1978) 2773.
- [30] J. Collins, *Foundations of Perturbative QCD*. Cambridge University Press. Cambridge, 2011.
- [31] T. Becher and M. Neubert, *On the Structure of Infrared Singularities of Gauge-Theory Amplitudes*, *JHEP* **06** (2009) 081, [[0903.1126](#)].
- [32] I. Feige and M. D. Schwartz, *Hard-Soft-Collinear Factorization to All Orders*, *Phys. Rev. D* **90** (2014) 105020, [[1403.6472](#)].
- [33] V. A. Smirnov and E. R. Rakhmetov, *The Strategy of regions for asymptotic expansion of two loop vertex Feynman diagrams*, *Theor. Math. Phys.* **120** (1999) 870–875, [[hep-ph/9812529](#)].
- [34] V. A. Smirnov, *Problems of the strategy of regions*, *Phys. Lett. B* **465** (1999) 226–234, [[hep-ph/9907471](#)].
- [35] A. Pak and A. Smirnov, *Geometric approach to asymptotic expansion of Feynman integrals*, *Eur. Phys. J. C* **71** (2011) 1626, [[1011.4863](#)].
- [36] G. Heinrich, S. Jahn, S. P. Jones, M. Kerner, F. Langer, V. Magerya et al., *Expansion by regions with pySecDec*, *Comput. Phys. Commun.* **273** (2022) 108267, [[2108.10807](#)].
- [37] E. Gardi, F. Herzog, S. Jones, Y. Ma and J. Schlenk, *The on-shell expansion: from Landau equations to the Newton polytope*, *JHEP* **07** (2023) 197, [[2211.14845](#)].
- [38] V. A. Smirnov, *Analytic tools for Feynman integrals*, vol. 250. Springer, 2012, [10.1007/978-3-642-34886-0](#).
- [39] B. Jantzen, A. V. Smirnov and V. A. Smirnov, *Expansion by regions: revealing potential and Glauber regions automatically*, *Eur. Phys. J. C* **72** (2012) 2139, [[1206.0546](#)].
- [40] A. V. Smirnov, N. D. Shapurov and L. I. Vysotsky, *FIESTA5: Numerical high-performance Feynman integral evaluation*, *Comput. Phys. Commun.* **277** (2022) 108386, [[2110.11660](#)].
- [41] T. Becher, A. Broggio and A. Ferroglia, *Introduction to Soft-Collinear Effective Theory*, vol. 896. Springer, 2015, [10.1007/978-3-319-14848-9](#).
- [42] A. Idilbi and T. Mehen, *On the equivalence of soft and zero-bin subtractions*, *Phys. Rev. D* **75** (2007) 114017, [[hep-ph/0702022](#)].
- [43] L. F. Abbott, *The Background Field Method Beyond One Loop*, *Nucl. Phys. B* **185** (1981) 189–203.
- [44] V. N. Popov, *Functional integrals in quantum field theory and statistical physics*. Reidel, 1984.
- [45] G. Falcioni, E. Gardi and C. Milloy, *Relating amplitude and PDF factorisation through Wilson-line geometries*, *JHEP* **11** (2019) 100, [[1909.00697](#)].
- [46] A. V. Belitsky, X. Ji and F. Yuan, *Final state interactions and gauge invariant parton distributions*, *Nucl. Phys. B* **656** (2003) 165–198, [[hep-ph/0208038](#)].

- [47] G. P. Korchemsky and A. V. Radyushkin, *Infrared Asymptotics of Perturbative QCD. Quark and Gluon Propagators*, *Sov. J. Nucl. Phys.* **45** (1987) 127.
- [48] A. V. Belitsky, A. S. Gorsky and G. P. Korchemsky, *Gauge / string duality for QCD conformal operators*, *Nucl. Phys. B* **667** (2003) 3–54, [[hep-th/0304028](#)].
- [49] P. M. Fishbane and J. D. Sullivan, *Asymptotic behavior of the vertex function in quantum electrodynamics*, *Phys. Rev. D* **4** (1971) 458–475.
- [50] A. H. Mueller, *Perturbative QCD at High-Energies*, *Phys. Rept.* **73** (1981) 237.
- [51] A. V. Belitsky, A. V. Smirnov and V. A. Smirnov, *MB tools reloaded*, *Nucl. Phys. B* **986** (2023) 116067, [[2211.00009](#)].
- [52] S. Catani, B. R. Webber and G. Marchesini, *QCD coherent branching and semiinclusive processes at large x* , *Nucl. Phys. B* **349** (1991) 635–654.
- [53] A. Grozin, J. M. Henn, G. P. Korchemsky and P. Marquard, *The three-loop cusp anomalous dimension in QCD and its supersymmetric extensions*, *JHEP* **01** (2016) 140, [[1510.07803](#)].
- [54] A. V. Belitsky, S. E. Derkachov, G. P. Korchemsky and A. N. Manashov, *Superconformal operators in $N=4$ superYang-Mills theory*, *Phys. Rev. D* **70** (2004) 045021, [[hep-th/0311104](#)].
- [55] D. J. Gross and S. B. Treiman, *Light cone structure of current commutators in the gluon quark model*, *Phys. Rev. D* **4** (1971) 1059–1072.